# Carbon Accumulation and Storage in a Temperate Coastal Lagoon under the Influence of Recent Climate Change (Northwestern Adriatic Sea)

**Roberta Guerra[1,2], Simona Simoncelli[3], and Andrea Pasteris[2,4]**

[1]Department of Physics and Astronomy, University of Bologna, Bologna, Italy, [2]Interdepartmental Research Centre for Environmental Sciences (CIRSA), University of Bologna, Ravenna Campus, 48123 Ravenna, Italy, [3]National Institute of Geophysics and Volcanology (INGV), Bologna, Italy, [4]Department of Biological, Geological, and Environmental Sciences (BiGeA), University of Bologna, Bologna, Italy.

Corresponding author: Roberta Guerra (roberta.guerra@unibo.it)

**Key Points:**

- The relative contribution of allochthonous marine-derived organic matter increased over the years reflecting local relative sea level
- Decreased contribution of autochthonous-derived organic matter from C3 vegetation is evident in the saltmarsh habitat since the 1950s
- Relative sea level rise influenced sedimentary organic matter although this effect was different between and within habitats

## Abstract

Pialassa Baiona is a shallow temperate coastal lagoon influenced by a variety of factors, including regional climate change and local anthropogenic disturbances. To better understand how these factors influenced modern organic carbon (OC) sources and accumulation, we measured OC as well as stable carbon isotopes ($\delta^{13}C$) in $^{210}Pb$-dated sediments within a vegetated saltmarsh habitat and a human impacted habitat. Relative Sea Level (RSL) at the nearby tide gauge station data and four different Sea Surface Temperature (SST) data sets were analyzed starting from 1900 to assess the potential effect of sea ingression and warming on the coastal lagoon sedimentary process. The source contribution calculated from the MixSIAR Bayesian model revealed a mixed sedimentary organic matter (OM) composition dominated by increasing marine-derived OM after the 1950s, parallel with decreasing autochthonous saltmarsh vegetation (*Juncus* spp.) in the saltmarsh habitat and riverine-estuarine-derived OM in the impacted habitat. RSL rise in the area (8.7±0.5 mm $yr^{-1}$ in the period 1900-2014) has been mainly driven by the land subsidence, especially during the central decades of the last century, enhancing the sea ingression in the lagoon. Annual SST anomalies present, starting from the eighties, a continuous warming tendency from 0.034±0.01 to 0.044±0.009°C $yr^{-1}$. No direct effect on sedimentary properties was detected; however, RSL influenced OM sediment properties, although this effect was different between the two habitats.



## Plain Language Summary

Coastal vegetated ecosystems (mangroves, saltmarshes, seagrasses) are highly efficient in removing carbon dioxide from the atmosphere through plant growth and thus play an important role in climate regulation, limiting the greenhouse effect. The term "blue carbon" has been devised to refer to carbon captured from the atmosphere and stored as organic matter in the sediments of these habitats. On the other hand, climate changes and human activities can affect coastal ecosystems and the quality and quantity of blue carbon. The goal of the present study was to analize how the characteristic of the organic matter stored in the sediment of a Mediterranean costal lagoon changed over the time from year 1850 to year 2010. These changes were compared with changes in sea water temperature and Relative Sea Level over the same period. Results showed that the importance of marine organic matter entering the lagoon from outside increased after the 1950s, while the contribution of organic matter produced inside the lagoon decreased. It is likely that Relative Sea Level, dominated by subsidence in the area, enhanced sea ingression and thus inputs of marine organic carbon. Such changes will continue to have an impact on the accumulation and storage of blue carbon.


## 1 Introduction

Carbon captured and stored in sediments from coastal vegetated habitats (wetlands, saltmarshes, tidal flats), where the rates of organic carbon (OC) accumulation from multiple sources is high, constitutes a relevant and active fraction in the global carbon sink, and plays an important role in climate regulation and mitigation (Kirwan and Mudd, 2012). However, a global inventory of this coastal 'blue carbon' storage remains a challenge, as observations of OC accumulation and stock in coastal ecosystems are labor intensive, expensive, scarce, and unevenly distributed, with few records even for relatively well-studied temperate areas in the Northern Hemisphere (Beaumont et al., 2014). Recent reviews (Duarte et al., 2005; Wilkinson et al., 2018) report a mean organic carbon accumulation rate of 151 g C $m^{-2}$ $yr^{-1}$ for saltmarshes (maximum 1720 g C $m^{-2}$ $yr^{-1}$), 41.4 g C $m^{-2}$ $yr^{-1}$ for lagoons (maximum 340 g C $m^{-2}$ $yr^{-1}$), and 62.9 g C $m^{-2}$ $yr^{-1}$ for coastal wetlands (maximum 335.8 g C $m^{-2}$ $yr^{-1}$) exceeding the mean burial rate of estuaries and continental shelves (17–45 g C $m^{-2}$ $yr^{-1}$).

The rate of accumulation of 'blue carbon', mostly stored in soil and sediments within coastal vegetated ecosystems, is sensitive to rapidly changing climate factors (e.g. warming, sea level rise, inundation frequency) and non climatic anthropogenic drivers (e.g. eutrophication, landscape development) (Arriola, 2017; Cuellar-martinez et al., 2019; Ewers Lewis et al., 2018; Kelleway et al., 2017; Kirwan and Mudd, 2012; Macreadie and

Saintilan, 2019; Macreadie et al., 2013; Negandhi et al., 2019; Pendleton et al., 2012; Rogers et al., 2019; Ruiz-fernández et al., 2018; Simpson et al., 2017). Between 20 and 90% of the existing area occupied by coastal vegetated ecosystems is projected to be lost at global level by 2100, depending on sea level rise projections and warming under future emission scenarios (IPPC, 2019).

Carbon stable isotopic composition ($\delta^{13}C$) in combination with supporting geochemistry, specifically the ratio of organic carbon to total nitrogen (C/N) and total organic carbon content (OC), have been used as tracers to differentiate sources of organic matter (OM) that characteristically accumulate in sediments of coastal vegetated habitats near the Westerschelde Estuary (SW Netherlands), in Massachusetts and South Carolina (USA) (Chen et al., 2016; Goñi et al., 2003; Middelburg et al., 1997), and in Australian coastal wetlands (Saintilan et al., 2013), as well as past sea level indicators in the Thames Estuary (Khan et al., 2015b), in tidal-dominated wetlands in North West Europe (Wilson, 2017), in a back-barrier lagoon system in New Jersey, USA (Kemp et al., 2012), and in Hudson Bay, Canada (Godin et al., 2017).

The signature of bulk organic sediment $\delta^{13}C$ and C/N analysis in sediment records in European coastal vegetated habitats is primarily to distinguish between OM derived from autochthonous C3 and C4 saltmarsh vascular vegetation (i.e. coastal blue carbon; $\delta^{13}C$ −12‰ to −30‰, C/N 5.80 to 41.10; Khan et al., 2015b), and allochthonous sources including fluvial and marine particulate organic matter (OM), the latter mainly derived from freshwater or marine phytoplankton ($\delta^{13}C$ −12‰ to −30‰, C/N 5 to 9; Lamb et al., 2006).

There is, however, little knowledge about the spatial and historical distribution, and the sources of sedimentary OM in coastal vegetated habitats in the Mediterranean Region. In this study, carbon stable isotopic composition ($\delta^{13}C$) and C/N ratios were measured, and Pb-210 chronology reconstructed in sediment cores from two contrasting habitats (a semi-natural saltmarsh habitat and an impacted habitat) within a coastal lagoon (Pialassa Baiona) connected to the Northwestern Adriatic Sea. This temperate shallow coastal ecosystem is subject to ongoing sea level rise, sea warming (Carbognin and Tosi, 2002; Cerenzia et al., 2016; Tsimplis et al., 2012; Mariano et al., 2021), land subsidence, hydrological alterations, coastal erosion, maintenance dredging, embankments (Airoldi et al., 2016; Guerra et al., 2009).

The objectives of this work were to investigate the changes in OM accumulation and sources, and to assess the climatic factors and local anthropogenic disturbances influencing the spatial and temporal changes in OM 'blue carbon' storage in this temperate coastal lagoon (Pialassa Baiona) located in the Mediterranean Region.

## 2 Materials and Methods

### 2.1 Study area

Pialassa Baiona is a temperate coastal lagoon (44° 280 N and 44°310 E) adjacent to the Northwestern Adriatic Sea (Figure 1). The area forms part of the Natura 2000 European network and is a wetland of international importance under the Ramsar Convention. The climate is hot-summer Mediterranean (Köppen-Geiger) with a continental influence, with a mean annual temperature of 14.1 °C and a maximum of 29.2°C (Antolini et al., 2016). Annual rainfall ranges from 650 mm to 696 mm, mainly from October to March (Mollema and Antonellini, 2012).

The lagoon consists of shallow water bodies of saline, brackish or fresh water wetlands (~0.5 m average depth) completely or partially isolated by levees and crossed by a dendritic network of artificial channels dug in 1850 (~5 m maximum depth). The inner channels converge into a main channel connected to sea through the shipway channel. Salinity in the lagoon (25–35 psu) is mainly controlled by tidal flushing through this channel into the channels network resulting in delayed tidal oscillation and low water exchange with the open sea. On average, the water covers an area of 10 $km^2$ with a tidal range of 0.3–1 m, and usually vast shallow areas emerge during low tides.

The northern area is composed of unvegetaed zones alternated with zones dominated by halophile species characteristic of temporarily inundated saltmarshes (*Juncus maritimus* and *Juncus acutus* and to a lesser

extent by *Salicornia* spp.; Merloni and Piccoli, 1999), with marginal areas with reedbeds of *Phragmites australis* (Ferronato et al., 2016).

The southern area is a subtidal habitat consisting of tidal wetlands separated by discontinuous artificial embankments receiving inputs from agriculture runoff, and urban and industrial wastewater discharges through the main inflow channel (Airoldi et al., 2016). Vegetation is sparse and mainly present on the embankments. This area has been subject to local anthropogenic disturbances (chemical and thermal pollution) resulting in higher than expected concentrations of mercury, chlorinated compounds and polycyclic aromatic hydrocarbons (PAHs) in sediments (Covelli et al., 2011; Guerra et al., 2014) and mussels (Capolupo et al., 2017), and alteration of the benthic community (Guerra et al., 2009; Ponti et al., 2011). The high THg concentrations found in the sediment of this area are in good agreement with the Hg inputs following the booming of petrochemical industry located near Pialassa Baiona lagoon in the mid-1950s. Chemical plants producing acetaldehyde and vinyl chloride from acetylene and using mercury salts as catalysts, released an estimated 100–200 tons of Hg directly into the southern area of the lagoon during the 1958–1978 period (Miserocchi et al., 1993). In 1973, wastewater treatment began, the acetaldehyde plant was shut down and the use of Hg catalysts in vinyl chloride and acetaldehyde production was drastically reduced and finally discontinued by 1991 (Fabbri et al., 1998).

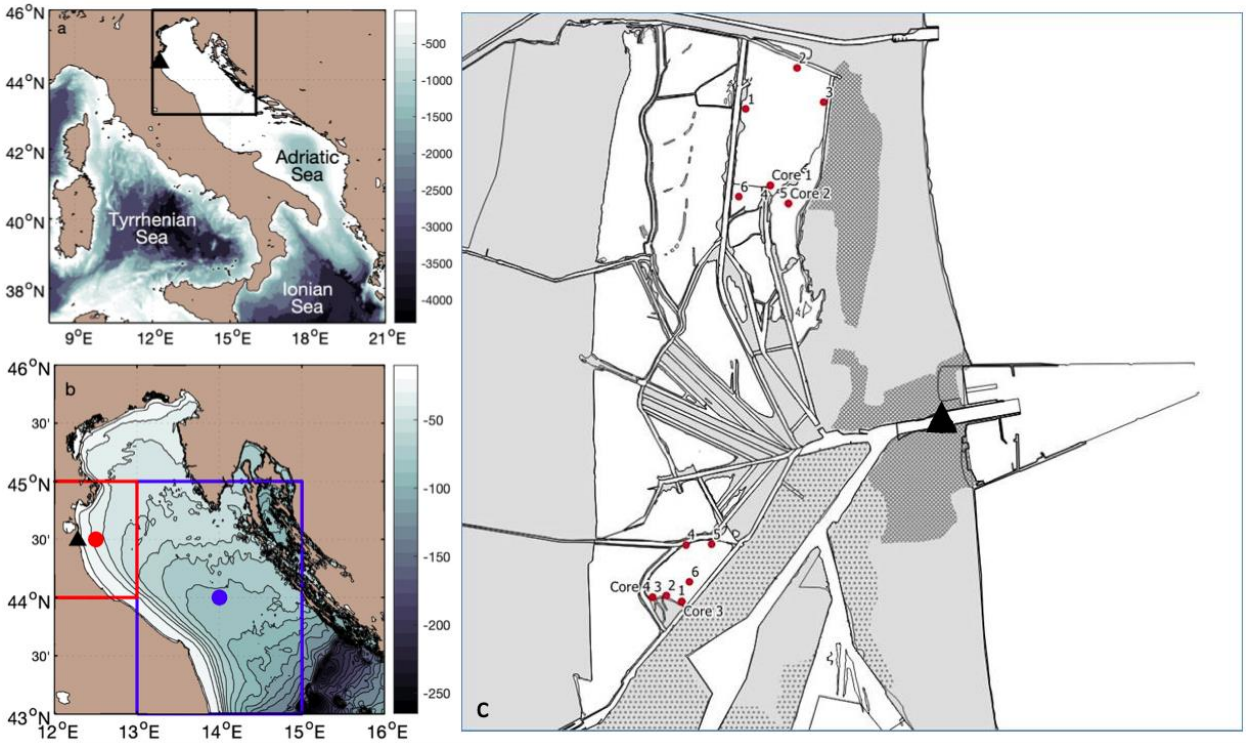


Figure 1. (a) Overview map and location of the study (black triangle) area overlain on the bathymetry from GEBCO Compilation Group (2019) GEBCO 2019 Grid. (b) Zoom in the Northern Adriatic Sea, corresponding to the black square in the left panel, and relative bathymetry. The red square and dot correspond to the HadlSST and COBE-SST mesh grid, while the blue square and dot correspond to the ERSST mesh grid. (c) Map of the Pialassa Baiona coastal lagoon and station locations of surface sediment samples and core samples in the saltmarsh habitat and impacted habitat. The black triangle indicates the Porto Corsini/Marina di Ravenna tide gauge location.

## 2.2 Sampling

Sampling took place in April and July 2008 at two contrasting habitats within Pialassa Baiona coastal lagoon: a) a saltmarsh habitat located northward in a relatively flat area with the presence of saltmarsh vegetation, and b) a human impacted habitat located southward close to anthropogenic source inputs (Figure 1). At each habitat, sediment cores were sampled at two random locations by inserting one cylindrical Plexiglas hand corer (5 cm diameter, 50 cm long) into the sediment to a depth of 20–25 cm. The cores were extruded in the field, sectioned into 1–2 cm intervals, and analyzed for total organic carbon (OC), total nitrogen (TN), carbon isotope ratio ($\delta^{13}C$) and dry bulk density (upper 20–25 cm). In addition, a composite of two sediment cores with no evidence of physical disturbance was taken at each habitat to reconstruct the chronology of sediment accummulation. These two cores were sampled within a 1-$m^2$ area within each habitat to attenuate variation due to spatial heterogeneity (Bernal and Mitsch, 2012). Composite core intervals were bulked together to provide satisfactory amounts, which were needed for effective $^{210}Pb$ dating and dry bulk density.

Additionally, a total of 12 surface sediment samples (0–5 cm) were collected with a stainless-steel grab sampler at six stations in the saltmarsh habitat and six stations at the impacted habitat for organic matter description (OC, TN and $\delta^{13}C$) (Figure 1).

155 2.3 Laboratory analysis

156 Freeze-dried sediment samples were treated with HCl (1.5 M) to remove inorganic carbon (carbonate).
157 Aliquots of approximately 20 mg were added into silver capsules for the measurement of total organic carbon
158 (OC), total nitrogen (TN), and carbon isotopes ($\delta^{13}C = [(^{13}C/^{12}C)_{sample}/(^{13}C/^{12}C)_{standard} - 1] \times 1{,}000$) using a
159 FINNIGAN Delta Plus XP mass spectrometer directly coupled to Thermo Fisher FLASH 2000 CHNS
160 Elemental Analyzer. OC and TN content were expressed as the weight percentage of dried sediment, and carbon
161 isotope results were reported in the standard delta notation (‰) with respect to the international standard Vienna
162 Pee Dee Belemnite (VPDB). Standard deviation based on replicates of reference standard (IAEA-CH7) was < ±
163 0.2‰.

164 For radiometric analysis, packed sediments (~40–50 g) were set aside for at least 21 days to allow $^{222}Rn$
165 ingrowth and to establish secular equilibrium between $^{226}Ra$ and its granddaughter $^{214}Pb$. The $^{210}Pb$ and $^{226}Ra$
166 activities were measured by γ-ray spectrometry, and the excess $^{210}Pb$ activity was estimated by subtracting the
167 $^{214}Pb$ from the total $^{210}Pb$ activity with self-absorption corrections (Cutshall et al., 1983). Detailed information
168 on the radiometric technique is provided in Guerra et al. (2019). The excess $^{210}Pb$ was used to determine ages of
169 sediment intervals using the 'simple' Constant Flux Constant Sedimentation model (CF-CS; Sanchez-Cabeza
170 and Ruiz-Fernandez, 2012). Sediment accumulation rates (SAR, cm $yr^{-1}$) and mass accumulation rates (MAR, g
171 $cm^{-2}$ $yr^{-1}$) were estimated from the profile of excess $^{210}Pb$ activity concentration versus sediment depth (cm)
172 and mass sediment depth (calculated using bulk density). An aliquot of sediment was dried at 60°C to measure
173 the water content and to calculate bulk density assuming a sediment density of 2.65 g $cm^{-3}$ and a water density
174 of 1.034 g $cm^{-3}$.

175 The OC accumulation rate (g OC $m^{-2}$ $yr^{-1}$) was estimated by multiplying the OC fraction (%OC/100) in
176 each core interval by the MAR (g $m^{-2}$ $yr^{-1}$). Total C stock (g C $m^{-2}$) was calculated by integrating OC
177 accumulation rates over the c.a. last century (1900–2008).

178 Total mercury (THg) was determined with a Perkin Elmer Optima 3200 XL inductively coupled plasma-
179 optical emission spectrometer coupled to a FIAS 400 hydride generation system following the US EPA method
180 6010C (USEPA, 2000). Sediments were digested with concentrated nitric acid ($HNO_3$, Suprapur, Merck; 65%)
181 and hydrochloric acid (HCl, Suprapur, Merk; 37%). QA/QC for THg analysis was carried out using sample
182 replicates, method blanks, and certified reference materials (CRMs, Marine Sediment PACS-2 and MESS-3
183 from NIST, USA). The accuracy of the instrument was consistently within their certified range (3.04±0.20, and
184 0.91±.009 μg $g^{-1}$, respectively), and all measured samples showed less than 10% deviation from CRMs.

185

186

187

188

189 2.4 Climatic data

190 Existing Sea Surface Temperature (SST) and Sea Level (SL) climatic data sets have been analyzed in
191 order to assess the main climatic characteristics and changes happened after 1900 in the study region and relate
192 them to the accumulation and variations in the pool of blue carbon through multivariate analysis.

193 One of the longest SL time series (1987–2014) available within the Northern Adriatic region has been
194 recorded at the Porto Corsini/Marina di Ravenna tide gauge station (44.49°N, 12.28°E), located nearby the
195 entrance to the Piallassa Baiona (Figure 1c), along the main shipway channel connected to the sea (Cerenzia et
196 al., 2016; Zerbini et al., 2017). The Relative SL (RSL) data, given by the combined effect of vertical land
197 movements and SL, used in the climatic analysis are the annual means (Figure 3) over the time period 1900–
198 2014 analyzed and provided by Cerenzia et al., (2016). They derive from different data sources and have been
199 properly homogenized relying upon the information on benchmarks and data overlaps. The three main RSL data
200 sources are: (1) the Permanent Service for Mean Sea Level (PSMSL) archive for the time period 1897–1922;

(2) the Hydrology Annals of Bologna for the 1934–1979 time period and (3) the Institute for Environmental Protection and Research (ISPRA) for the period 1980–2014.

The centennial RSL change presents anomalous rate of increase (8.5±0.2 mm $yr^{-1}$) within the Northern Adriatic and the Northern Mediterranean region. Cerenzia et al., (2016) found out that land subsidence represents the main cause of local RSL rise measured by the tide gauge due to a total land lowering from 1.8 to 0.2 m above sea level in the time period 1897–2014.

The rate of absolute SL change during the last decades, obtained by subtracting the rate of land subsidence from the rate of RSL change, is equal to 2.2±1.3 mm $yr^{-1}$, consistently with other tide gauge observations nearby (i.e. Venice, Trieste) and the estimate of 3 mm $yr^{-1}$ computed from altimetry in the region from Bonaduce et al., (2016). Another long-term sea level trend estimate from Bruni et al., (2019) at Porto Corsini/Marina di Ravenna tide gauge gives a value of 1.25±0.16 mm $yr^{-1}$ over the time period 1873–2016.

Sea Surface Temperature gridded data sets covering the time period 1900–2018 have been retrieved from three global climatic data products with the aim to obtain a robust estimate of the long term temperature variation of the sea water entering and exiting the coastal lagoon under investigation to be used for the multivariate analysis. Three global monthly SST data sets have been considered: (1) the HadISST from Met Office Hadley Centre for Climate Prediction and Research; (2) the ERSST from NOAA National Centers for Environmental Information and (3) the COBE-SST from the Japan Meteorological Agency (JMA). These products might not fully capture regional details, as highlighted by (Li et al., 2019) thus a fourth, most recent and accurate regional satellite-based data set (Pisano et al., 2016) distributed by the Copernicus Marine Environment Monitoring Service (CMEMS) has been considered as the reference to validate the three global products and select the most representative of the area for the successive analysis. The CMEMS SST is the longest satellite SST time series (1982–2018) at 4 km resolution for the Mediterranean Basin and it is spatially complete, accurate, homogeneous and stable, i.e. free of spurious trends, all essential characteristics for products usability for climate applications. The main characteristics of the considered SST data sets have been summarized in Table 1 and detailed in the supporting information.

Table 1. Main characteristics of the SST data sets used and displayed in Figure 3.

| **SST Product** | **Reference** | **Time Coverage** | **Time resolution** | **Space resolution [degrees]** |
|---|---|---|---|---|
| **HadlSST** | (Rayner et al., 2003) | 1882 onwards | monthly | 1x1 |
| **ERSST** | (Huang et al., 2017) | 1854 onwards | monthly | 2x2 |
| **COBE-SST** | (Ishii et al., 2005) | 1891 onwards | monthly | 1x1 |
| **CMEMS REP L4** | (Pisano et al., 2016) | 1981–2018 | daily mean | 0.0417x0.0417 |

The closest sea grid point to the study area (Figure 1) has been selected from each global data set to first inspect the time series. HadlSST and COBE-SST sea grid points are coincident and the grid cell includes the coastal strip [12–13°E; 44–45°N] up to approximately the 40 m bathymetric (red square in Figure 1b). The ERSST grid cell (blue square in Figure 1b) is wider than the others, due to its coarser resolution and it encloses a central area of the Northern Adriatic sea [13–15°E; 43–45°N], which does not include the considered coastal strip. The CMEMS SST sea grid points falling inside the HadlSST and COBE-SST grid cell have been selected from daily fields to compute monthly averages and represent the best SST estimate of the coastal area under investigation.

A preliminary consistency analysis of the monthly SST time series has been conducted and is provided in the supporting information (Figure S1). The outcome suggests a consistency among the centennial SST data sets and CMEMS SST and their potential usability to characterize the long term SST variations of the domain under investigation.

SST annual averages and relative anomalies have been computed subtracting from each time series its relative time average (i.e. 1900-2014 for the centennial datasets, 1982-2018 for CMEMS SST). The resulting annual SST anomalies are displayed in Figure 3 together with the annual RSL values from Cerenzia et al., (2016).

The correlation between the annual anomalies from the centennial SST datasets and the reference CMEMS SST have been computed over the time period 1982–2018 in order to select the most correlated one to be used in the successive multivariate analysis. The correlation is highly significant and it is equal to 0.85 for COBE-SST, 0.86 for HadlSST and 0.88 for ERSST. The correlation among all four SST annual anomalies and the annual RSL has been computed too and it results minimum for COBE-SST (0.42) and maximum for CMEMS SST (0.63), while it is equal to 0.54 and 0.55 for HadlSST and ERSST respectively.

The analysis of the available centennial datasets suggested to select the ERSST annual averages for the successive analyses on sediment OM data due to its highest correlation with both CMEMS SST and RSL, even if its grid mesh does not include the area under investigation (Figure 1). The reason could depend from the largest availability of in situ data within the ERSST widest grid box on which the gridded data product relies, making its estimate more robust.

### 2.5 Multivariate statistical analysis

The constrained ordination method of redundancy Analysis (RDA, Legendre and Legendre, 2012) was employed to evaluate the relation between sediment OM data (response variables) and the climatic ERSST and RSL data (explanatory variables). The analysis was carried out using the R package VEGAN. The overall significance of the RDA model and of the single explanatory variables was tested using the permutest() and anova.rda() functions of VEGAN, which are based on permutation methods. Due to the availability of RSL and SST data, the period prior to 1897 and the periods 1922–1935, 1941–1945 and 1990–1994 could not be included in the RDA. Organic matter data and climatic variables were further averaged during the period comprised by each core section. Four distinct RDA were performed, one for each core. Correlation between single explanatory and response variables and between variables and RDA axes was quantified and tested using the Pearson's r coefficient.

## 3 Results

### 3.1 $^{210}$Pb geochronology

The excess $^{210}$Pb profile showed a decreasing trend with depth, and activities ranged from 0.8 to 33.5 Bq kg$^{-1}$ in the saltmarsh habitat, and from 14.4 to 58.7 Bq kg$^{-1}$ in the impacted habitat, with an overall mean value of 23.1±17.0 Bq kg$^{-1}$. The period covered by each sedimentary core is longer than 100 years, and the time span from 1900 to 2008 (Figure S2). The average sediment accumulation rates (SAR, 0.15±0.06 cm yr$^{-1}$ and 0.21±0.06 cm yr$^{-1}$) and mass accumulation rate (MAR, 0.16±0.07 and 0.17±0.06 g cm$^{-2}$ yr$^{-1}$) were comparable in the saltmarsh habitat and the impacted habitat, respectively.

The modern (last decades to century) sediment chronologies estimated from the excess $^{210}$Pb CF-CS model were compared to the profiles of THg concentration (Table S1). Generally, the THg concentration increased from low near background regional values in the bottom layers to the maximum values in the sub-surface layers followed by a rapid decrease towards the upper layers (Figure S3). THg concentrations were <0.12 mg kg$^{-1}$ up to 9 cm and 12 cm depth in the saltmarsh and impacted habitat cores, respectively (1950±4

and 1953±4). The onset of THg was recorded in the middle layers of the impacted habitat core and the saltmarsh habitat core (11 and 8 cm, respectively; year 1957±3). The highest values of THg were found in the middle layers of the impacted habitat core (6–9 cm, from year 1967±3 to 1977±2), where the concentrations of THg were always higher than 20 mg $kg^{-1}$, with a maximum value of 25.3 mg $kg^{-1}$ (7 cm, year 1977±2).

The mean differences of geochronology (1958 and 1978) between the results from excess $^{210}$Pb and THg are 1.0±0.7 years and 2.5±5.1 years, respectively. The relatively consistent estimation results of $^{210}$Pb and THg indicated the geochronology was valid, although the biggest uncertainty (6.1 years) was found in the saltmarsh core (Table S1).

### 3.2 Elemental and isotopic composition of sedimentary organic carbon

The OC content, C/N ratio and $\delta^{13}$C in the surface sediment ranged from 1.04 to 2.62%, from 6.92 to 10.99, and from −21.87 to −18.21‰ in the saltmarsh habitat, and from 0.68 to 2.62%, from 6.98 to 11.1, and from −26.81 to −20.91‰ in the impacted habitat (Table S2). $\delta^{13}$C values were significantly enriched in the saltmarsh habitat when compared to the impacted habitat (−20.06±1.31 ‰ and −23.34±2.00 ‰; $p < 0.007$), whereas C/N ratios did not show any significant difference between the surface sediments from the saltmarsh and impacted habitats.

On the basis of $^{210}$Pb chronology and historical Hg concentrations, three time periods were defined: before 1957, 1957–1977, and after 1977.

In the saltmarsh habitat cores, OC content ranged from 0.38 to 1.38% and from 0.22 to 1.31% (core 1 and core 2), and from 2.06 to 3.74% and from 2.53 to 3.94% in the impacted habitat cores (core 3 and core 4); C/N ratio varied from 6.62 to 12.73 and from 6.32 to 15.80 in the saltmarsh habitat (core 1 and core 2), and from 6.64 to 10.56 and 6.74 11.33 in the impacted habitat (core 3 and core 4). The range of variation of $\delta^{13}$C was −22.19 to −19.19 ‰ and −20.25 to −17.74 ‰ in the saltmarsh habitat (core 1 and core 2, respectively), and −26.26 to −22.09 ‰ and −27.21 to 22.76 ‰ in the impacted habitat (core 3 and core 4, respectively) (Figure 2 and Table S3).

In the saltmarsh habitat, $\delta^{13}$C values were slightly but significantly depleted in the sediments deposited before the 1950s than in recent years (1980s–2008) (−21.15±0.60 ‰ and −19.41±0.21 ‰ , $p < 0.001$ ) in core 1; conversely, core 2 did not display any significant difference over time (−19.12±0.55 ‰ and −19.18±1.03 ‰, respectively). In the impacted habitat, $\delta^{13}$C values in recent sediments (−22.54±0.39 ‰ in core 3 and −23.61±0.62 ‰ in core 4) displayed a marked and significant enrichment in comparison to the 1960s–1970s intermediate layers (−24.82±0.69 ‰, $p < 0.001$ in core 3, and −25.84±1.43 ‰, $p = 0.003$ in core 4) and older layers deposited prior to the 1950s (−25.49±0.73 ‰, $p < 0.001$ in core 3 and −25.62±0.77 ‰, $p = 0.002$ in core 4).

In the saltmarsh habitat, C/N ratios did not display any significant increase from recent sediments (1980s–2008) to the older layers deposited prior to the 1950s in core 1 (7.98±1.20 and 9.04±1.56) and in core 2 (8.38±1.05 and 9.71±3.47). In the impacted habitat, C/N ratios slightly but significantly increased from recent sediments (1980s–2008) to the older layers deposited prior to the 1950s both in core 3 (8.11±0.61 and 9.44±1.20, respectively; $p = 0.038$) and core 4 (7.85±0.70 and 9.41±0.79, respectively; $p = 0.004$).

Accumulation rates of OC ranged from 8.0 to 14.6 g $m^{-2}$ $yr^{-1}$ and 4.5 to 15.5 g $m^{-2}$ $yr^{-1}$ in the saltmarsh habitat (core 1 and core 2), and from 32.4 to 57.6 g $m^{-2}$ $yr^{-1}$, and 22.2 to 54.7 g $m^{-2}$ $yr^{-1}$ in the impacted habitat (core 3 and core 4). In the saltmarsh habitat, OC accumulation rates were slightly but significantly higher in intermediate and recent sediments (1960s–2008) than in the older layers deposited prior to the 1950s both in core 1 (12.97±1.35 g $m^{-2}$ $yr^{-1}$ and 9.35±1.23 g $m^{-2}$ $yr^{-1}$, respectively; $p = 0.003$) and in core 2 (13.79±1.25 and 8.40±3.69 g $m^{-2}$ $yr^{-1}$, respectively; $p = 0.047$). In the impacted habitat, there were no significant differences in OC accumulation rates between the older, intermediate and recent layers in core 3 (44.82±8.30, 39.04±4.48, and 41.63±4.68 g $m^{-2}$ $yr^{-1}$, respectively). In core 4, OC accumulation rates were significantly higher in the older

layers deposited prior to the 1950s than in intermediate (1960s–1970s) and recent sediments (1980s–2008) (43.57±7.20, 24.51±2.11, and 33.78±8.20 g $m^{-2}$ $yr^{-1}$; p <0.001 and p = 0.034, respectively) (Figure 2).

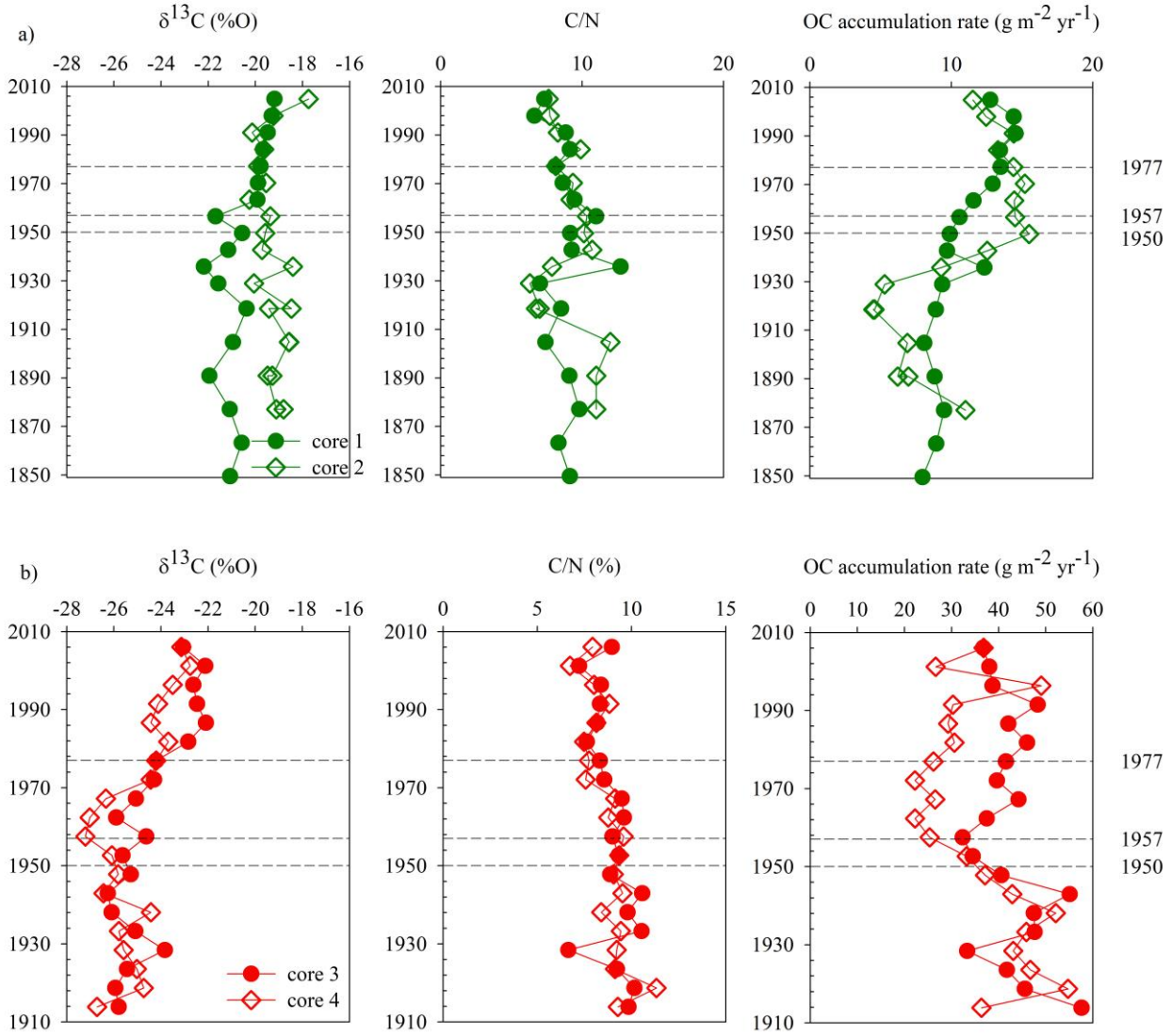


Figure 2. Vertical distributions of stable carbon isotope ($\delta^{13}C$), C/N ratio, and OC accumulation rates in recent deposited sediments (1978–2008), intermediate layers (1957–1977) and older layers (deposited prior to the 1950s) within Pialassa Baiona coastal lagoon from a) the saltmarsh habitat and b) the impacted habitat.

### 3.3 Climatic site characterization

The RSL time series over the considered 1900–2014 time period (Figure 3) is characterized by a total variation of 98.4 cm with a continuous rise starting from the '40s until present, characterized by a steep increase from the '40s to the '70s. The RSL trend is equal to 8.7±0.5 mm yr−1, which reduces to 7.0±1.4 mm $yr^{-1}$ in the most recent 1982–2014 time period.

Cerenzia et al. (2016) highlight the dominant role of land movement on the RSL rise in this area and report a natural subsidence trend of about 6 mm $yr^{-1}$ in the time period 1897–1950 followed by a noticeable increase over the period 1950–1970, corresponding to a rate of about 24 mm $yr^{-1}$. Bruni et al., (2019) also

describe a moderate RSL rising tendency before 1940, a steep increase from the ‘40 to the 70s and its significant reduction after 1980.

The effect of human activities in the study area is thus predominant in the area with respect to SL rise, especially from the ‘40s until the 1970s, when subsidence due to groundwater withdrawal from surface aquifers and gas extraction have superimposed onto the regional tectonic component. As a consequence the sea water ingression within the coastal lagoon increased in time, modulated by tidal flow.

SST annual anomalies (Figure 3) appear mainly negative during the first two decades (1900–1920), they fluctuate approximately between ±0.5°C from 1920 to 1970 with the most pronounced ERSST negative anomalies during the 1940s. Between 1970 and the early 1980s the anomalies become mainly negative, but since that period the SST start a continuous warming tendency characterized by always positive anomalies approximately after the year 2000. Consistently, CMEMS SST anomalies appear mostly negative before the year 2000 and positive afterwards.

The total ERSST variation over the 1900–2018 time period is equal to 1.0°C with a constant increase of 0.009±0.002°C $yr^{-1}$. SST increases mainly from the early 1980s, thus the linear trends in the time period 1982–2018 is provided too: ERSST trend is equal to 0.034±0.010°C yr−1 and CMEMS SST is 0.044±0.009°C $yr^{-1}$. The latest value is comprised within the estimates by Pisano et al. (2020) for the whole Mediterranean Sea (0.041±0.006°C $yr^{-1}$) and the Adriatic Sea (0.045±0.007°C $yr^{-1}$).

Starting from the ‘80s the effect of subsidence slowed down due to mitigation effects but SL rise continues at a rate of about 2.2 mm ±1.3 mm $yr^{-1}$ (1990-2011; Cerenzia et al., 2016) and contemporary SST increases with unprecedented rate.

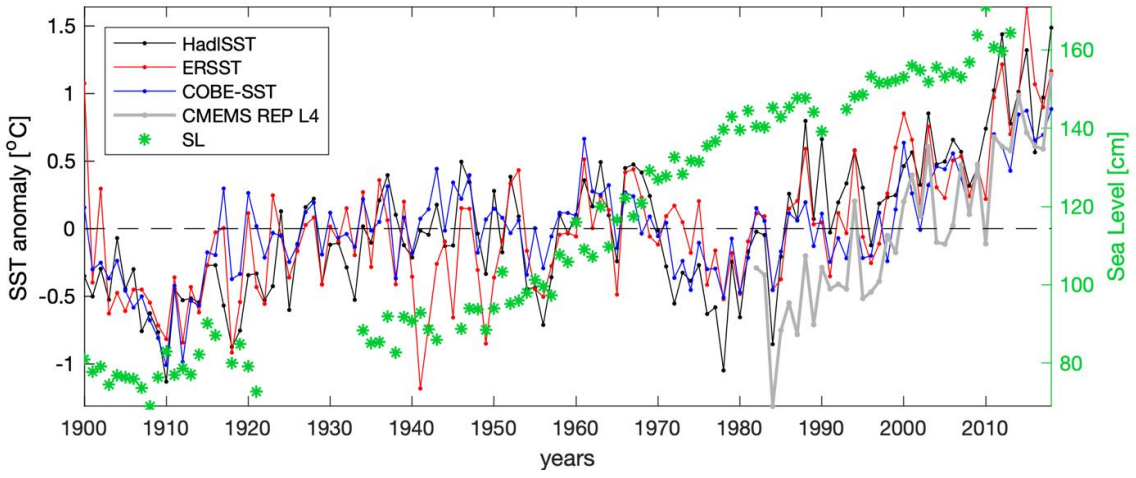


Figure 3. Annual mean time series of RSL (1900–2014) at the Porto Corsini tide gauge (Cerenzia et al., 2016) and SST anomalies (1900–2018) from three global data products (HadlSST, ERSST, COBE-SST) and a reference regional data product from CMEMS (1982–2018). SST data products characteristics are summarized in Table 1.

## 4 Discussion

### 4.1 Organic matter sources

Coastal wetlands ecosystems represent the convergence of terrestrial and marine systems, hence stable carbon isotopes ($\delta^{13}C$) and the ratio of organic carbon to total nitrogen (C/N) values of these environments will

depend on the relative contributions of carbon derived from saltmarsh vascular vegetation, phytoplankton, seagrasses, algae, and particulate organic carbon (POC) transported by rivers and tides (Lamb et al., 2006). $\delta^{13}C$ and C/N together are able to differentiate sources of OM that accumulate in coastal depositional records, specifically between C3 and C4 vegetation and freshwater and marine organic matter (Kemp et al., 2012, 2010; Khan et al., 2015b; Oreska et al., 2018).

In order to estimate the relative contribution of different OM sources supplied to and stored in sediments of Pialassa Baiona coastal lagoon, we combined $\delta^{13}C$ and C/N values of saltmarsh habitat cores ($n$ = 38), impacted habitat cores (n = 40), and saltmarsh and impacted habitat surface sediments ($n$ = 6 and $n$ = 6, respectively) (Table S2 and S3 in the supporting information). The $\delta^{13}C$, C/N and OC composition of modern sediments (c.a. last century) in the two habitats of the lagoon generally indicated their spatial and temporal distribution (Figure 3 and Figure 4). Despite this distinct pattern, a significant positive correlation ($p < 0.0001$, $n$ = 88) between contents of OC and TN was observed with a strong linear relationship and a close to zero intercept (TN = 0.01312*OC + 0.0048; $r^2$ = 0.9459). This clearly indicates common OM sources in the two habitats, and suggests that nitrogen in sediments was predominantly bound to sedimentary OC, thus is probably in an organic form (Hedges et al., 1986).

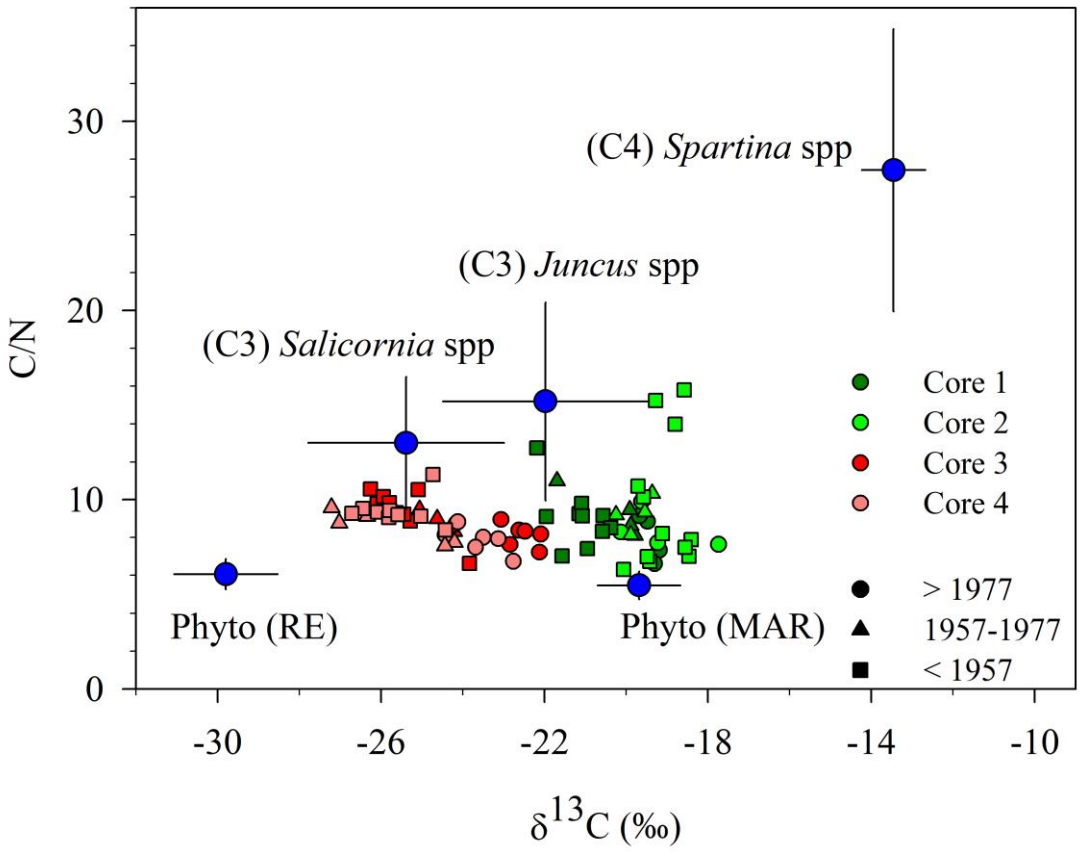


Figure 4. Plot of the stable OC isotopic compositions ($\delta^{13}C$) and atomic carbon: nitrogen ratios (C/N) in recent deposited sediments (1980s–2008), intermediate layers (1960s–1980s) and older layers (prior to the 1950s) from the saltmarsh habitat (core 1 and core 2) and the impacted habitat (core 3 and core 4) within Pialassa Baiona coastal lagoon (Gebrehiwet et al., 2008; Guerra et al., 2013; Hughes and Sherr, 1983; Kelleway et al., 2017; Kemp et al., 2012, 2010; Lamb et al., 2006). The compositions of five possible OM sources: marsh (C3) vascular vegetation (*Juncus* spp. and *Salicornia* spp.), marsh (C4) *Spartina* spp., riverine-estuarine phytoplankton (Phyto (RE)), marine phytoplankton (Phyto (MAR)), are plotted to show the relative contribution of allochthonous and autochthonous OM.

The C/N ratio has been used as effective index to characterize predominant sources of OM in coastal marshes and lagoons (Cloern et al., 2002; Khan et al., 2015b; Meyers, 1994; Wilson, 2017). Previous studies reported C/N ratios for C3 and C4 saltmarsh vegetation OM that are typically >12, whereas values for marine OM are <8; intermediate values are thought to be mixed. C/N values varies little between the saltmarsh and impacted habitats sediments and is consistently <10 with very few exceptions (Figure 3 and Figure 4). The C/N ratio indicates that the sedimentary OM in the saltmarsh and impacted habitats had a mixed source of freshwater- and marine-derived OM, and the freshwater source of OM was mainly distributed in the impacted habitat, while the saltmarsh habitat was dominated by marine source OM. Despite the overall low C/N values, still a slight but consistent increasing trend from recent layers (1980s–2008) to the pre 1950s sediments can be identified in the impacted habitat (Figure 3b). Significant changes in C/N typically occur in early stages of OM microbial degradation (Dai et al., 2005), and this may have resulted in in situ lower surface sediment C/N compared to the older deposited layers.

Carbon isotope signatures clearly allocated sediments in two distinct groups, with enriched $\delta^{13}C$ values found in the saltmarsh habitat, and relatively depleted $\delta^{13}C$ values in the impacted habitat lying between values for corresponding marine and riverine-estuarine end-members (Figure 4). These $\delta^{13}C$ values infer a change in OM sources from the saltmarsh to the impacted habitat, and reflect contributions from mixed sources of sedimentary OM suggesting that allochthonous freshwater/riverine sources may have a local influence in the impacted habitat, while allochthonous marine sources seem to predominate in the saltmarsh habitat. The $\delta^{13}C$ values of the saltmarsh and impacted habitats partially overlay the isotopic signatures of saltmarsh vegetation of a C3 photosynthetic pathway origin, which have a $\delta^{13}C$ extent of −29.88 to −20.2 ‰ and a C/N of 9.70 to >20 (Khan et al., 2015a; Lamb et al., 2006). So far C4 saltmarsh plants are either absent or have been recently introduced in North European saltmarshes (Preston et al., 2002); to our knowledge there is no record of C4 Spartina spp. presence in Pialassa Baiona coastal lagoon in the scientific and grey literature.

Locally produced (autochthonous) biomass is generally considered to contribute significantly to the total OC pool in saltmarsh sediments (Chen et al., 2016). Among saltmarsh vascular vegetation, species of the genus Juncus is the prevailing C3 high marsh plant of Pialassa Baiona coastal lagoon (Merloni and Piccoli, 1999). Allochthonous sources are the marine-derived OM, imported through tidal flow from the main channel connecting to the sea, and the riverine-estuarine derived OM, brought in by the main inflow channel located on the southern edge of the lagoon, while *Juncus*-derived OM is likely produced in situ, and thus represents an autochthonous source in the sedimentary OM of the saltmarsh and impacted habitats.

To estimate the proportional contribution of the different sources to the sediment OM in each of the cores we applied MixSIAR, a Bayesian mixing model framework implemented as an open-source R package (Stock et al, 2018). MixSIAR, and mixing models in general, require tracer data that characterize the chemical or physical traits of both the sources and the mixtures; these traits are assumed to predictably transfer from sources to mixtures through a mixing process. In the present application $\delta^{13}C$ and C/N are used as tracers. Marine phytoplankton, riverine/estuarine phytoplankton and Juncus spp. are considered the potential sources while sediments are the mixtures.

Tracer values for marine phytoplankton ($\delta^{13}C$: −19.7±1.0 ‰; C/N: 5.5±0.7) and for riverine/estuarine phytoplankton ($\delta^{13}C$: −29.8±1.3 ‰; C/N: 6.1±0.8) were obtained from Tesi et al. (2007) and Guerra et al. (2013). Values for *Juncus* spp. ($\delta^{13}C$: −22.0±2.5 ‰; C/N: 15.2±5.2) were obtained from Gebrehiwet et al. (2008) and Kelleway et al. (2017).

Regardless of the tracers or mixing system considered, all mixing model applications are rooted in the same fundamental mixing equation:

$$\mathbf{Y_j} = \sum_{\mathbf{k}} \mathbf{p_k}\, \boldsymbol{\mu}^{\mathbf{s}}_{\mathbf{jk}}$$

where the mixture tracer value, Yj , for each of j tracers is equal to the sum of the k source tracer means, μsjk, multiplied by their proportional contribution to the mixture, pk.

MixSIAR, through the application of Markov chains Monte Carlo sampling, estimates the probability density function of each pk value, i.e. the proportional contribution of each source to the final mixture. Statistics like mean and standard deviation are then calculated from this estimated distribution. Bayesian mixing models improve upon simpler linear mixing models by explicitly taking into account uncertainty in source values. MixSIAR, in particular, has the ability to incorporate categorical and continuous covariates to explain variability in the mixture proportions and offers several options for error parametrization.

In our analysis, two categorical covariates, core and time period, were taken into account. Error was assumed as "residual only", in accordance with the indications of Stock et al. (2016) for the application of mixing models to sediment sourcing. The probability density functions of the proportional contributions of the three sources to the sediment OM are shown in Figure S4, separately for each core and time period. Means, standard deviations and percentiles of the same distributions are reported in Table S4.

The marine-derived OM increased from ~50% in the sediments deposited prior to the 1950s to ~70% in recent decades (1980s–2008) in the saltmarsh habitat. Similarly, marine-derived OM increased from ~15% in the sediments deposited prior to the 1950s to ~40% in recent decades (1980s–2008) in the impacted habitat. Riverine-estuarine OM sources accounted for <10% and ~50 % of sedimentary OM in the saltmarsh and impacted habitats over the last century; these sources decreased from ~60% in the pre 1950s period to ~40% in recent decades (1980s–2008), while marine-derived OM contribution increased simultaneously after the 1950s within the impacted habitat. These findings indicate that the relative contribution of marine-derived OM to recent sediments are larger than in sediments deposited prior to the 1950s, and this contribution is by ~30% higher in saltmarsh habitat sediments than in the impacted habitat. The explanation of the increasing contribution of tidally-derived OM is related to an increasing inflow of sea water into the lagoon over the last decades supported by the positive RSL trend recorded by the tide gauge.

$\delta^{13}C$ signatures and C/N showed that an important fraction of sedimentary OM stored in sediment within Pialassa Baiona coastal lagoon is derived from the autochthonous C3 saltmarsh plant Juncus spp. Overall, this fraction is slightly higher within the saltmarsh habitat, where C3 saltmarsh vegetation-derived OM comprised on average ~33% of the OM sedimentary pool when compared to the ~26% fraction in the impacted habitat sediments. The mixing model evidenced a change in C3 saltmarsh vegetation OM contribution from ~40% to ~20% in the sediment records from the saltmarsh habitat in the pre 1950s period to recent decades (1980s–2008) concomitant with the increased marine-derived OM contribution from the 1950s forward, and from ~30 to ~25% in the impacted habitat, respectively. The most plausible explanation is that $\delta^{13}C$, OC and C/N geochemistry of sediments varied in relation to mixing of the autochthonous OM from in situ C3 saltmarsh vegetation with an increased contribution from allochthonous particulate OM from marine sources, which in turn, is controlled primarily by tidal inundation.

### 4.2 Relationship between organic matter and climatic variables

Redundancy analysis (RDA) was employed to determine if the observed spatial and temporal variability in sedimentary OM data was related to regional climatic changes (Figure 5). RDA model, tested by using the permutest procedure, is highly significant for all the cores except core 2 (Figure 5b). RDA axes account from 38% (core 4) to 66% (core 1) of the total variation, thus a large fraction of the differences in sediment OM properties among core sections is not explained by the RSL and SST (Figure 5, Table S5). The first axis (RDA1) accounts for 86% (core 3) to 97% (core 1) of the explained variance and was positively correlated with both RSL and SST, although RSL had higher scores on this axis. The second axis (RDA2), which accounts only for 3% to 14% of explained variance, was mostly related to SST. As a consequence, RDA1 can be interpreted as the conjunct variation of RSL and SST, while RDA2 as the fraction of SST variation that is not related to the RSL. However, SST presents little independent explanatory power since its effect, tested using the anova.rda procedure, is in all cases not significant. On the other hand the effect of RSL is highly significant in the three cores (1, 3 and 4) where the RDA model is also highly significant.

Recent years (after 1977) show high values on RDA1 axis (except for core 2 not significant) well separated from older years (before 1957), which are instead characterized by low values. Years 1957–1977 score intermediate values and overlap with both recent and older years. This result reflects the steady rise in RSL and SST changes over the last century (Figure 3): low RDA1 scores before 1957 when both RSL and SST rise are low, intermediate RDA1 scores between 1957 and 1977 when SST is not increasing while RSL rapidly increases mainly under the effect of subsidence, while high RDA1 scores appear after 1977 when both RSL and SST increase.

TN was positively correlated with RDA1 and C/N ratio was negatively correlated with RDA1 in all four cores. On the other hand, the relation between other OM variables and RDA1 was not consistent among the four cores. OC content was positively correlated with RDA1 and TN content in the saltmarsh habitat (cores 1 and 2), while independent from RDA1 in the impacted habitat (cores 3 and 4). Correlation between OC accumulation rate and RDA1 was positive in the saltmarsh habitat, negative in the impacted habitat, although correlation was significant only for cores 1 and 4. $\delta^{13}C$ was positively correlated with RDA1 in all cores with the exception on core 2 (saltmarsh habitat).

In summary RDA suggested that climatic variables, in particular RSL due to the cumulated effect of land movement and SL rise, influenced OM properties of the sediments. However, the effect of this influence was not consistent between the two habitats, and differences were observed even between cores from the same habitat.

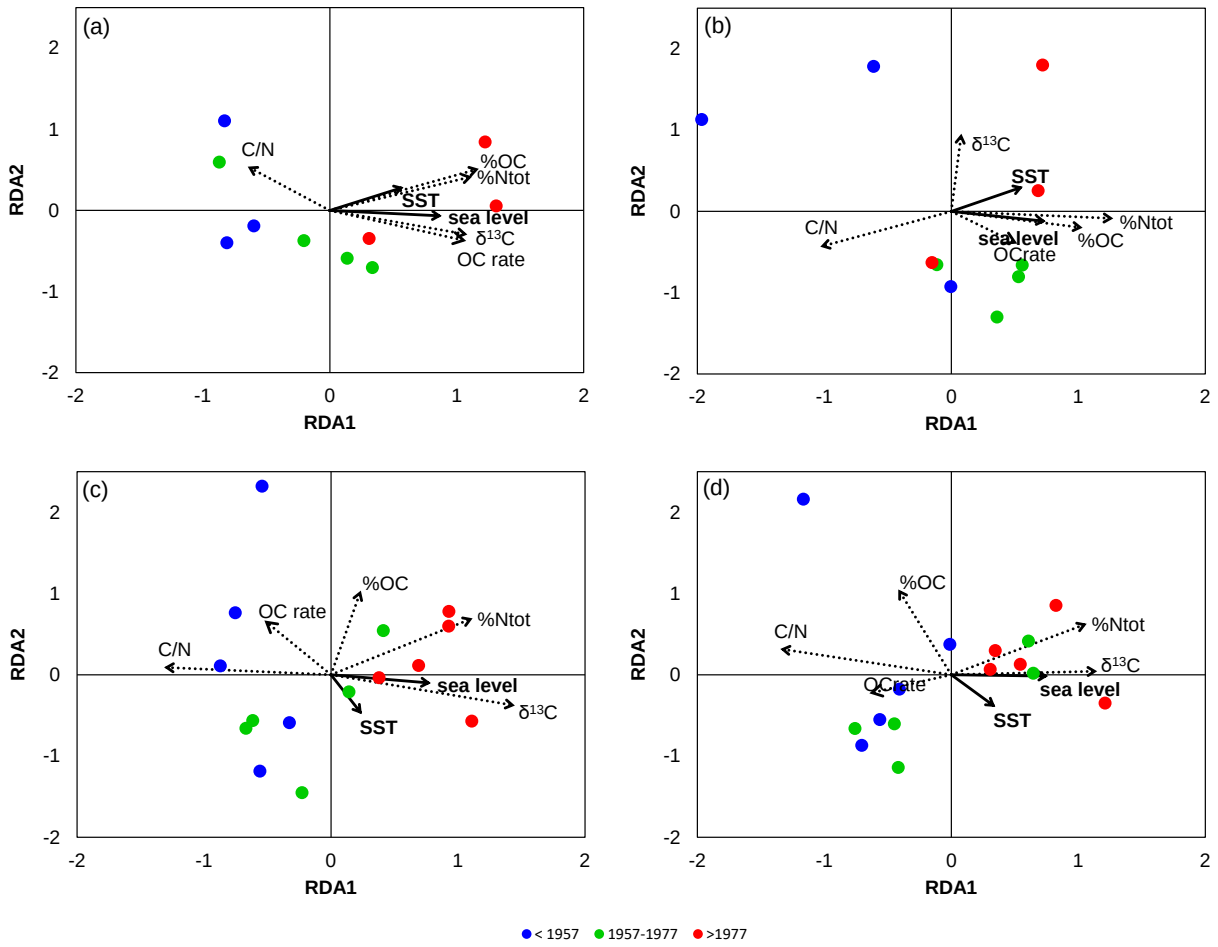


Figure 5. Plot of RDA analysis with response sedimentary OM variables (OC, $\delta^{13}C$, OC accumulation rates) and explanatory regional climatic variables (RSL and SST): (a) saltmarsh habitat core 1, (b) saltmarsh habitat core 2, (c) impacted habitat core 3 and (d) impacted habitat core 4.

### 4.3 Organic matter accumulation

Core dating using excess $^{210}Pb$ confirmed that the sediment bed has accreted due to sediment accumulation in the saltmarsh and impacted habitats over the last century. The differences in geochronology resulting from excess $^{210}Pb$ and THg can be attributed to complex depositional conditions and biogeochemical cycling with northward migration of Hg causing a delayed THg peak (Covelli et al., 2011; Fabbri et al., 2001; Trombini et al., 2003).

Pb-210 derived SARs are comparable with published accretion rates measured within Oregon tidal saline wetlands (0.13–0.29 cm $yr^{-1}$) and Long Island Sound (0.1–0.36 cm $yr^{-1}$) (Peck et al., 2020; Hill and Anisfeld, 2015), in microtidal coastal wetlands in the Gulf of California and the Caribbean Sea (0.04–0.65 cm $yr^{-1}$) (Ruiz-fernández et al., 2018), and within Venice lagoon under rising sea level, subsidence and increasing frequency of high tides flooding called ‘acqua alta’ (0.13–0.44 cm $yr^{-1}$) (Bellucci et al., 2007).

Salt marshes are vulnerable and dynamic systems that can extend landward in response to lateral erosion and accrete vertically by accumulating sufficient materials to compensate for rising sea level (Fagherazzi et al., 2020; Kirwan and Megonigal, 2013; Mariotti and Carr, 2014). Sediment accretion is further promoted by the presence of halophytic plants producing OM, which in turn, can be partially buried favoring net sediment accumulation (Cahoon et al., 2021).

To explore whether Pialassa Baiona lagoon is a net depositional or erosional area, excess $^{210}$Pb (Bq cm$^{-2}$) inventories were estimated at sediment core habitats according to a standard technique (Appleby and Oldfield, 1992), and then compared to the annual atmospheric flux of $^{210}$Pb within the latitudinal range 40-50°N (0.0155±0.0075 Bq cm$^{-2}$ yr$^{-1}$) (Baskaran, 2011). The mean excess $^{210}$Pb inventory for sediment cores at the saltmarsh and impacted habatitats is 0.37 ± 0.27 Bq cm$^{-2}$, which is lower than the steady state inventory of atmospheric $^{210}$Pb (0.50±0.24 Bq cm$^{-2}$) at 40–50°N, and thus the study area is not net depositional.

Averaged SAR over the period ~1900–2010 (~0.2 mm yr$^{-1}$) is lower than the local RSL (Cerenzia et al., 2016) increase owing to rapid land subsidence in the 1950–1970, thus indicating the accretion balance is negative and the area is less likely to keep pace with the ongoing SL rise. SL rise scenarios for the year 2100 and relative inundations map for the subsiding Northern Adriatic coastal plain, predict that the coastal area under investigation will be most probably submerged by that time (Antonioli et al., 2017; Mariano et al., 2021).

Although OC accumulation rates averaged over 1900s–2008 are lower than the averages for tidal wetlands soils and salt mash sediments (Ouyang and Lee, 2014; Wang et al., 2019), they compare well to mean OC rate in modern sediments (ca < 200 yrs) in coastal and inland aquatic eosystems (Wilkinson et al., 2018). In terms of carbon sequestration, our data suggests that modern sediments in the study area are similar to recently deposited sediments soils in vegetaded U.K. salt marsh habitats, as well as salt marshes in the Blackwater, Sheldth, and Guadiana estuaries (Table 2).

The variation of modern OC accumulation rates between the two habitats is remarkable, with the highest values found in the impacted habitat located in the southern lagoon, an area that historically received allochthonous inputs of OC and nutrients from agriculture runoff and wastewater discharges through the main inflow channel draining an intensely cultivated watershed (Giordani et al., 2005). Lower OC values were found in the saltmarsh habitat located in the northern area of the lagoon, distal from the main freshwater and anthropic inputs from inland activities.

Before the 1950s, OC accumulation rates in the impacted habitat were on average higher and negatively correlated with RSL, a trend confirmed as statistically significant for core 3. This could be explained by a decrease in the amount of suspended solids entering the inflow channels from the watershed. While there are no direct measurements available for the time period under consideration, this appears to be in line with the recorded hydrological changes in the area (Buscaroli et al., 2011).

In the nineteenth century, the inland of Pialassa Baiona, which is now entirely reclaimed agricultural land, was predominantly formed up of wetlands, which were connected to the lagoon though channels. The Lamone River, which previously flowed directly into the Adriatic Sea north of Bialassa Baiona, was redirected to flow into the wetlands southwest of the lagoon in 1846, to reclaim agricultural land by filling the wetlands with sediments brought by the river. When the southern wetlands were filled, the river was shifted northward, finally returning to run directly into the Adriatic Sea north of Pialassa Baiona at the turn of the 1950s. As a result of the reclamation process, the lagoon was gradually cut off from the Lamone river's suspended solids flow.

Our hypothesis is that the balance between increasing sedimentation of marine OM (due to RSL rise) and decreasing riverine OM was somewhat negative in the impacted habitat, resulting in a decrease in OC accumulation rate over time. Conversely, the saltmarsh habitat was already excluded from riverine OM contributions at the turn of the nineteenth century, and thus increased sedimentation of marine OM resulted in an increase of OC accumulation rate.

A plausible explanation of the lower OC accumulation rates found in this habitat could be attributed to the predominance of marine phytoplankton sources increasing with RSL rise over the last century with a minor contribution from prevailing C3 saltmarsh vegetation *(Juncus* spp.) as evidenced by the isotopic $^{13}$C signals and the MixSIAR model outputs. Marine phytoplankton predominantly consists of macromolecules (pigments, lipids, carbohydrates, and aminoacids) that show a steady decline through the water column into the sediments (Hama et al., 2004; Wakeham et al., 1997) in contrast to intrinsically refractory components (for example lignin and lipid biomarkers) typical of terrestrial angiosperms (Hedges and Mann, 1979), and of marine and wetland

vascular plants including Juncus spp (Clifford et al., 1995; Goñi and Thomas, 2000; Klap et al., 2000) that are selectively preserved and accumulated into the sedimentary OC pool of coastal systems (Bianchi et al., 2018; Goñi et al., 1998; Kuzyk et al., 2008; Tanner et al., 2010, 2007).

OC storage and sink capacity of blue carbon ecosystems, including saltmarshes, are impacted at spatial and temporal scales by rapidly changing climate and anthropogenic factors, comprising SL rise, land subsidence, warming, hydrological alterations, and landscape development (Ouyang and Lee, 2014; Tan et al., 2020), and these disturbances resulted in estimated areal losses of 0.2–7% $yr^{-1}$ at global level (Spivak et al., 2019). Human-caused and climatic changes have also affected the physical environment of the Pialassa Baiona coastal lagoon and its adjacent areas throughout the previous century, particularly in the middle of the 1900s due to the combination of SL rise and fast subsidence rate, resulting in changes in OM accumulation and sources in their sediments.

### 4.4 Carbon stock

For the 1900–2008 period, the carbon stock estimated from the OC accummulation rates is 1253±12 g C $m^{-2}$ for the saltmarsh habitat, and 4223±40 g C $m^{-2}$ for the impacted habitat. Overall, the estimated amount of OC stored in the two habitats are 1223±24 g C $m^{-2}$ and 3800±20 g C $m^{-2}$, respectively, of which ~30% are 'blue carbon' from in situ C3 saltmarsh vascular vegetation.

Between habitat variability has important implications for attempts to characterize blue carbon based on modern environmental conditions (c.a. last century). Our results suggest that contemporary changes in the RSL and allochthonous sources are likely to affect both C stocks and OC accumulation rates. That is, we found approximately threefold differences in OC accumulation rates and C stock between the saltmarsh habitat and the impacted habitat.

Over a century scale (1900–2008), the total C pool stored in the sediments is 7379 Mg C and 13682 Mg C in the saltmarsh and impacted habitats (589 ha and 324 ha, respectively), totaling 21061 Mg C corresponding to an area of ~10 $km^2$. According to the global dataset of carbon dioxide emissions (World Bank, 2019), Italy per capita $CO_2$ emissions went from 2.20 in 1960 to 7.11 tons in 2010. If we consider the averaged country's national $CO_2$ emissions per capita over this period (6.40 tons), the estimated C pool stored in the two habitats of the Pialassa Baiona amounted to ~77000 Mg $CO_2$, or the equivalent of ~12000 individuals Italian peoples $CO_2$ emissions per year. These estimates, while small in terms of national CO2 emissions (338 Mt $CO_2$; Friedlingstein et al., 2019), are equivalent to 3% of the annual estimated CO2 emissions from fossil fuel use and combustion of the closest town (Ravenna) (INEMAR-ER, 2019).

## 4 Conclusions

OC accumulation rates, OC sources and carbon stock were estimated in $^{210}$Pb-dated sediment cores from a salt marsh habitat and an impacted habitat within Pialassa Baiona coastal lagoon (Northwestern Adriatic Sea) and paralleled to the temporal trends and changes of SST and RSL in the region. The main findings of this work can be summarized as follows:

- OC accumulation rates showed a contrasting pattern from the 1950s forward, with a significant increasing trend in the saltmarsh habitat and a decreasing trend in the impacted habitat, though significant only in one core;

- Allochthonous marine-derived OM sources showed a consistent increase in 1980s–2008 when compared to the pre 1950s period, parallel with a decreased contribution from autochthonous saltmarsh vegetation (*Juncus* spp.) reflecting an increased sea water inflow into the lagoon as confirmed by RSL positive trend in the area;

- RSL change in the coastal region has been continuously increasing due to the sum of prevailing land subsidence of both natural and anthropogenic origin, and the SL rise. It has been faster during the central decades of the last century, due to the land lowering caused by ground fluids extraction, while it slowed down during the last decades, when subsidence returned to natural rates after the adoption of mitigation measures.

- SST analysis indicate quite stable SST anomalies until the 1960s, negative anomalies in the 1970s, a rapid and continuous SST increase from the eighties with a trend between $0.034\pm0.010$°C $yr^{-1}$ and $0.044\pm0.009$°C $yr^{-1}$.

- A direct effect of SST on sedimentary C has not been detected, however RL rise and SST warming are not independent, due to a contribution of thermal expansion to SL rise ranging from 30% to 40% approximately (Storto et al., 2019).

- Substantial differences have been observed between the saltmarsh and the impacted habitats as to sediment OM composition and sources, rate of accumulation, as well as the temporal trends of these properties and their relationship with climatic variables. Even cores collected few meters apart within the same habitat were appreciably different.

- The estimated total C pool stored in sediments equals ~3% of the annual estimated $CO_2$ emissions from the nearby town.

The findings of this study confirm that Pialassa Baiona coastal lagoon is an important coastal blue carbon ecosystem in sequestering carbon from atmospheric CO2 emissions. However, with an annual loss rate of 1–2% between 1980 and 2000 (Spivak et al., 2019) under increasing SL rise and warming, this trend is likely to compromise the capacity of coastal vegetated habitats like Pialassa Baiona coastal lagoon for atmospheric CO2 uptake and storage, unless proper management and coastal protection is implemented. According to SL rise scenarios and inundations map this coastal vegetated habitat is likely to be submerged by 2100, and thus specific measures should also be implemented to mitigate sea ingression.

There are significant data gaps on carbon stocks in coastal vegetated habitats in the Mediterranean Region, and the characteristic variability of these habitats, is a significant challenge to the goal of a global coastal blue carbon inventory. Further research and mapping of C stock and greenhouse gas fluxes including methane ($CH_4$) in coastal vegetated habitats at regional and national level is strongly recommended.

## Acknowledgments and Data

This study was supported by the University of Bologna strategic research grant FinQuer (2007–2009). Mapping, core sampling and handling was graciously conducted by M. Ponti. E. Fetter and S. Righi assisted with laboratory work. We thank Marco Olivieri for providing mean SL data from Cerentia et al. (2016). The Mediterranean Sea Surface CMEMS SST dataset used in this paper is freely distributed through http://marine.copernicus.eu and identified as SST_MED_SST_L4_REP_OBSERVATIONS_010_021 in the CMEMS catalogue.

The data sets reported in Table S2 and Table S3 (Supplementary Information) are freely available and accessible at SEANOE, https://doi.org/10.17882/73534.

## References


Adams, C.A., Andrews, J.E., Jickells, T., 2012. Nitrous oxide and methane fluxes vs. carbon, nitrogen and phosphorous burial in new intertidal and saltmarsh sediments. Sci. Total Environ. 434, 240–251. https://doi.org/10.1016/j.scitotenv.2011.11.058

Airoldi, L., Ponti, M., Abbiati, M., 2016. Conservation challenges in human dominated seascapes : The harbour and coast of Ravenna. Reg. Stud. Mar. Sci. 8, 308–318.

Antolini, G., Auteri, L., Pavan, V., Tomei, F., Tomozeiu, R., Marletto, V., 2016. A daily high-resolution gridded climatic data set for Emilia-Romagna , Italy , during 1961 – 2010. Int. J. Clim. 36, 1970–1986. https://doi.org/10.1002/joc.4473

Antonioli, F., Anzidei, M., Amorosi, A., Lo Presti, V., Mastronuzzi, G., Deiana, G., De Falco, G., Fontana, A., Fontolan, G., Lisco, S., Marsico, A., Moretti, M., Orrù, P.E., Sannino, G.M., Serpelloni, E., Vecchio, A., 2017. Sea-level rise and potential drowning of the Italian coastal plains: Flooding risk scenarios for 2100. Quat. Sci. Rev. 158, 29–43. https://doi.org/10.1016/j.quascirev.2016.12.021

Appleby, P.G., Oldfield, F., 1992. Application of 210Pb to sedimentation studies, in: I. Ivanovich, & R.S.H. (Ed.), Uranium Series Disequilibrium: Applications to Earth, Marine, and Environmental Sciences. Oxford University Press, Oxford, pp. 731–778.

Arriola, J.M., 2017. Variations in carbon burial and sediment accretion along a tidal creek in a Florida salt marsh. Limnol. Ocean. 62, 2017, 62, S15–S28. https://doi.org/10.1002/lno.10652

Baskaran, M., 2011. Po-210 and Pb-210 as atmospheric tracers and global atmospheric Pb-210 fallout: A Review. J. Environ. Radioact. 102, 500–513. https://doi.org/10.1016/j.jenvrad.2010.10.007

Beaumont, N.J., Jones, L., Garbutt, A., Hansom, J.D., Toberman, M., 2014. The value of carbon sequestration and storage in coastal habitats. Estuar. Coast. Shelf Sci. 137, 32–40. https://doi.org/10.1016/j.ecss.2013.11.022

Bellucci, L.G., Frignani, M., Cochran, J.K., Albertazzi, S., 2007. Pb and 137 Cs as chronometers for salt marsh accretion in the Venice Lagoon e links to flooding frequency and climate change 97. https://doi.org/10.1016/j.jenvrad.2007.03.005

Bertoni, W., Brighenti, G., Gambolati, G., Gatto, P., Ricceri, G., Vuillermin, F., 1988. Risultati Degli Studi e Delle Ricerche Sulla Subsidenza di Ravenna. Ravenna.

Bianchi, T.S., Cui, X., Blair, N.E., Burdige, D.J., Eglinton, T.I., Galy, V., 2018. Centers of organic carbon burial and oxidation at the land-ocean interface. Org. Geochem. 115, 138–155. https://doi.org/10.1016/j.orggeochem.2017.09.008

Bonaduce, A., Pinardi, N., Oddo, P., Spada, G., Larnicol, G., 2016. Sea-level variability in the Mediterranean Sea from altimetry and tide gauges. Clim. Dyn. 47, 2851–2866. https://doi.org/10.1007/s00382-016-3001-2

Boski, A.T., Moura, D., Correia, V., Martins, H., Camacho, S., Journal, S., Issue, S., Proceedings, N., 2021. Postglacial Organic Carbon Accumulation in Coastal Zones - a Possible Cause for Varying Atmospheric $CO_2$ levels. Preliminary Data from SW Portugal. J. Coast. Res. SI 39, 1864–1868.

Bruni, S., Zerbini, S., Raicich, F., Errico, M., 2019. Rescue of the 1873 – 1922 high and low waters of the Porto Corsini / Marina di Ravenna ( northern Adriatic , Italy ) tide gauge. J. Geod. 93, 1227–1244.

Buscaroli, A., Dinelli, E., Zannoni, D. 2011. Geohydrological and environmental evolution of the area included among the lower course of the Lamone River and the Adriatic coast. EQA – Environmental quality / Qualité de l'Environnement / Qualità ambientale, 5, 11-22.

Caçador, I., Costa, A.L., Vale, C., 2004. Carbon storage in tagus salt marsh sediments. Water, Air, Soil Pollut. Focus 4, 701–714. https://doi.org/10.1023/B:WAFO.0000028388.84544.ce

Cahoon, D.R., McKee, K.L., Morris, J.T., 2021. How Plants Influence Resilience of Salt Marsh and Mangrove Wetlands to Sea-Level Rise. Estuaries and Coasts 44, 883–898. https://doi.org/10.1007/s12237-020-00834-w

Calvo-Cubero, J., Ibáñez, C., Rovira, A., Sharpe, P.J., Reyes, E., 2014. Changes in nutrient concentration and carbon accumulation in a mediterranean restored marsh (Ebro Delta, Spain). Ecol. Eng. 71, 278–289. https://doi.org/10.1016/j.ecoleng.2014.07.023

Capolupo, M., Franzellitti, S., Kiwan, A., Valbonesi, P., Dinelli, E., Pignotti, E., Birke, M., Fabbri, E., 2017. A comprehensive evaluation of the environmental quality of a coastal lagoon (Ravenna, Italy): Integrating chemical and physiological analyses in mussels as a biomonitoring strategy. Sci. Total Environ. 598, 146–159. https://doi.org/10.1016/j.scitotenv.2017.04.119

Carbognin, L., Tosi, L., 2002. Interaction between Climate Changes , Eustacy and Land Subsidence in the North Adriatic Region , Italy 1, 38–50.

Cerenzia, I., Putero, D., Bonsignore, F., Galassi, G., Olivieri, M., Spada, G., 2016. Historical and recent sea level rise and land subsidence in Marina di Ravenna , northern Italy. Ann. Geophys. 59, 1–12. https://doi.org/10.4401/ag-7022

Chen, S., Torres, R., Goñi, M.A., 2016. The Role of Salt Marsh Structure in the Distribution of Surface Sedimentary Organic Matter. Estuaries and Coasts 39, 108–122. https://doi.org/10.1007/s12237-015-9957-z

Clifford, D.J., Carson, D.M., McKinney, D.E., Bortiatynski, J.M., Hatcher, P.G., 1995. A new rapid technique for the characterization of lignin in vascular plants: thermochemolysis with tetramethylammonium hydroxide (TMAH). Org. Geochem. 23, 169–175. https://doi.org/10.1016/0146-6380(94)00109-E

Cloern, J.E., Canuel, E.A., Harris, D., 2002. Stable carbon and nitrogen isotope composition of aquatic and terrestrial plants of the San Francisco Bay estuarine system. Limnol. Oceanogr. 47, 713–729. https://doi.org/10.4319/lo.2002.47.3.0713

716 Couto, T., Duarte, B., Caçador, I., Baeta, A., Marques, J.C., 2013. Salt marsh plants carbon storage in a temperate Atlantic estuary
717 illustrated by a stable isotopic analysis based approach. Ecol. Indic. 32, 305–311. https://doi.org/10.1016/j.ecolind.2013.04.004
718 Covelli, S., Emili, A., Acquavita, A., 2011. Benthic biogeochemical cycling of mercury in two contaminated northern Adriatic coastal
719 lagoons. Cont. Shelf Res. J. 31, 1777–1789. https://doi.org/10.1016/j.csr.2011.08.005
720 Cuellar-martinez, T., Ruiz-fernández, A.C., Sanchez-cabeza, J., Pérez-bernal, L., Sandoval-gil, J., 2019. Relevance of carbon burial
721 and storage in two contrasting blue carbon ecosystems of a north-east Paci fi c coastal lagoon. Sci. Total Environ. 675, 581–593.
722 https://doi.org/10.1016/j.scitotenv.2019.03.388
723 Curado, G., Rubio-Casal, A.E., Figueroa, E., Grewell, B.J., Castillo, J.M., 2013. Native plant restoration combats environmental
724 change: Development of carbon and nitrogen sequestration capacity using small cordgrass in European salt marshes. Environ. Monit.
725 Assess. 185, 8439–8449. https://doi.org/10.1007/s10661-013-3185-4
726 Cutshall, N.H., Larsen, I.L., Olsen, C.R., 1983. Direct analysis of $^{210}$Pb in sediment samples: Self-absorption corrections. Nuclear
727 Instruments and Methods in Physics Research 206, 309–312.
728 Dai, J., Sun, M.Y., Culp, R.A., Noakes, J.E., 2005. Changes in chemical and isotopic signatures of plant materials during degradation:
729 Implication for assessing various organic inputs in estuarine systems. Geophys. Res. Lett. 32, 1–4.
730 https://doi.org/10.1029/2005GL023133
731 Diesing, M., Thorsnes, T., Rún Bjarnadóttir, L., 2021. Organic carbon densities and accumulation rates in surface sediments of the
732 North Sea and Skagerrak. Biogeosciences 18, 2139–2160. https://doi.org/10.5194/bg-18-2139-2021
733 Duarte, C.M., Middelburg, J.J., Caraco, N., 2005. Major role of marine vegetation on the oceanic carbon cycle. Biogeosciences 1, 1–8.
734 https://doi.org/10.5194/bg-2-1-2005
735 Ewers Lewis, C.J., Carnell, P.E., Sanderman, J., Baldock, J.A., Macreadie, P.I., 2018. Variability and Vulnerability of Coastal 'Blue
736 Carbon' Stocks: A Case Study from Southeast Australia. Ecosystems 21, 263–279. https://doi.org/10.1007/s10021-017-0150-z
737 Fabbri, D., Vassura, I., Sun, C., Snape, C.E., Mcrae, C., Fallick, A.E., 2003. Source apportionment of polycyclic aromatic
738 hydrocarbons in a coastal lagoon by molecular and isotopic characterisation. Mar. Chem. 84, 123–135. https://doi.org/10.1016/S0304-
739 4203(03)00135-X
740 Fagherazzi, S., Mariotti, G., Leonardi, N., Canestrelli, A., Nardin, W., Kearney, W.S., 2020. Salt Marsh Dynamics in a Period of
741 Accelerated Sea Level Rise. J. Geophys. Res. Earth Surf. 125, 1–31. https://doi.org/10.1029/2019JF005200
742 Fennessy, M.S., Ibánez, C., Calvo-Cubero, J., Sharpe, P., Rovira, A., Callaway, J., Caiola, N., 2019. Environmental controls on carbon
743 sequestration, sediment accretion, and elevation change in the Ebro River Delta: Implications for wetland restoration. Estuar. Coast.
744 Shelf Sci. 222, 32–42. https://doi.org/10.1016/j.ecss.2019.03.023
745 Ferronato, C., Falsone, G., Natale, M., Zannoni, D., Buscaroli, A., Vianello, G., Vittori Antisari, L., 2016. Chemical and pedological
746 features of subaqueous and hydromorphic soils along a hydrosequence within a coastal system (San Vitale Park, Northern Italy).
747 Geoderma 265, 141–151. https://doi.org/10.1016/j.geoderma.2015.11.018
748 Friedlingstein, P., Jones, M.W., O'Sullivan, M., Andrew, R.M., Hauck, J., Peters, G.P., Peters, W., Pongratz, J., Sitch, S., Le Quéré,
749 C., Bakker, D.C.E., Canadell, J.G., Ciais, P., Jackson, R.B., Anthoni, P., Barbero, L., Bastos, A., Bastrikov, V., Becker, M., Bopp, L.,
750 Buitenhuis, E., Chandra, N., Chevallier, F., Chini, L.P., Currie, K.I., Feely, R.A., Gehlen, M., Gilfillan, D., Gkritzalis, T., Goll, D.S.,
751 Gruber, N., Gutekunst, S., Harris, I., Haverd, V., Houghton, R.A., Hurtt, G., Ilyina, T., Jain, A.K., Joetzjer, E., Kaplan, J.O., Kato, E.,
752 Goldewijk, K.K., Korsbakken, J.I., Landschützer, P., Lauvset, S.K., Lefèvre, N., Lenton, A., Lienert, S., Lombardozzi, D., Marland,
753 G., McGuire, P.C., Melton, J.R., Metzl, N., Munro, D.R., Nabel, J.E.M.S., Nakaoka, S.-I., Neill, C., Omar, A.M., Ono, T., Peregon,
754 A., Pierrot, D., Poulter, B., Rehder, G., Resplandy, L., Robertson, E., Rödenbeck, C., Séférian, R., Schwinger, J., Smith, N., Tans,
755 P.P., Tian, H., Tilbrook, B., Tubiello, F.N., R. van der Werf, G., Wiltshire, A.J., Zaehle, S., 2019. Global Carbon Project. (2019).
756 Supplemental data of Global Carbon Budget 2019 (Version 1.0) [Data set]. Global Carbon Project. https://doi.org/10.18160/gcp-2019
757 Gebrehiwet, T., Koretsky, C.M., Krishnamurthy, R. V., 2008. Influence of Spartina and Juncus on saltmarsh sediments. III. Organic
758 geochemistry. Chem. Geol. 255, 114–119. https://doi.org/10.1016/j.chemgeo.2008.06.015
759 Giordani, G., Viaroli, P., Swaney, D.P., Murray, C.N., Zaldívar, J.M., Marshall Crossland, J.I., 2005. Pialassa Baiona Lagoon,
760 Ravenna, Nutrient fluxes in transitional zones of the Italian coast. LOICZ Reports & Studies No. 28. LOICZ, Textel, the Netherlands.
761 Godin, P., Macdonald, R.W., Kuzyk, Z.Z.A., Goñi, M.A., Stern, G.A., 2017. Organic matter compositions of rivers draining into
762 Hudson Bay: Present-day trends and potential as recorders of future climate change. J. Geophys. Res. Biogeosciences 122, 1848–
763 1869. https://doi.org/10.1002/2016JG003569
764 Goñi, M.A., Ruttenberg, K.C., Eglinton, T.I., 1998. A reassessment of the sources and importance of land-derived organic matter in
765 surface sediments from the Gulf of Mexico. Geochim. Cosmochim. Acta 62, 3055–3075. https://doi.org/10.1016/S0016-
766 7037(98)00217-8
767 Goñi, M.A., Teixeira, M.J., Perkeya, D.W., 2003. Sources and distribution of organic matter in a river-dominated estuary (Winyah
768 Bay, SC, USA). Estuar. Coast. Shelf Sci. 57, 1023–1048. https://doi.org/10.1016/S0272-7714(03)00008-8
769 Goñi, M.A., Thomas, K.A., 2000. Sources and transformations of organic matter in surface soils and sediments from a tidal estuary
770 (North Inlet, South Carolina, USA). Estuaries 23, 548–564. https://doi.org/10.2307/1353145
771 Guerra, R., Pasteris, A., Lee, S.-H., Park, N.-J., Ok, G., 2014. Spatial patterns of metals, PCDDs/Fs, PCBs, PBDEs and chemical
772 status of sediments from a coastal lagoon (Pialassa Baiona, NW Adriatic, Italy). Mar. Pollut. Bull. 89, 407–416.
773 https://doi.org/10.1016/j.marpolbul.2014.10.024
774 Guerra, R., Pasteris, A., Ponti, M., 2009. Impacts of maintenance channel dredging in a northern Adriatic coastal lagoon. I : Effects on
775 sediment properties , contamination and toxicity. Estuar. Coast. Shelf Sci. 85, 134–142. https://doi.org/10.1016/j.ecss.2009.05.021

Guerra, R., Pistocchi, R., Vanucci, S., 2013. Dynamics and sources of organic carbon in suspended particulate matter and sediments in Pialassa Baiona lagoon (NW Adriatic Sea, Italy). Estuar. Coast. Shelf Sci. 135, 24–32. https://doi.org/10.1016/j.ecss.2013.06.022

Hama, T., Yanagi, K., Hama, J., 2004. Decrease in molecular weight of photosynthetic products of marine phytoplankton during early diagenesis. Limnol. Oceanogr. 49, 471–481. https://doi.org/10.4319/lo.2004.49.2.0471

Hedges, J., Mann, D., 1979. The characterization of plant tissues by their lignin oxidation products. Geochim. Cosmochim. Acta 43, 1803–1807. https://doi.org/https://doi.org/10.1016/0016-7037(79)90028-0

Hedges, J.I., Clark, W.A., Quay, P.D., Richey, J.E., Devol, A.H., Santos, U.M., 1986. Composition and fluxes of particulate organic material in the Amazon River. Limnol. Oceanogr. 31, 717–738.

Hensel, P.F., Day, J.W., Pont, D., 1999. Wetland vertical accretion and soil elevation change in the Rhone River Delta, France: The importance of riverine flooding. J. Coast. Res. 15, 668–681.

Hill, T.D., Anisfeld, S.C., 2015. Coastal wetland response to sea level rise in Connecticut and New York. Estuar. Coast. Shelf Sci. 163, 185–193. https://doi.org/10.1016/j.ecss.2015.06.004

Huang, B., Thorne, P.W., Banzon, V.F., Boyer, T., Chepurin, G., Lawrimore, J.H., Menne, M.J., Smith, T.M., Vose, R.S., Zhang, H.M., 2017. Extended reconstructed Sea surface temperature, Version 5 (ERSSTv5): Upgrades, validations, and intercomparisons. J. Clim. 30, 8179–8205. https://doi.org/10.1175/JCLI-D-16-0836.1

Hughes, E.H., Sherr, E.B., 1983. Subtidal food webs in a georgia estuary: δ13C analysis. J. Exp. Mar. Bio. Ecol. 67, 227–242. https://doi.org/10.1016/0022-0981(83)90041-2

INEMAR-ER, 2019. AGGIORNAMENTO DELL'INVENTARIO REGIONALE DELLE EMISSIONI IN ATMOSFERA DELL'EMILIA-ROMAGNA RELATIVO ALL'ANNO 2015. Rapporto finale. https://www.arpae.it/it/temi-ambientali/aria/inventario-emissioni/inventario_emissioni_2015.pdf.

IPPC, 2019. IPCC, 2019: Summary for Policymakers, in: Pörtner, H.-O., Roberts, D.C., Masson-Delmotte, V., Zhai, P., Tignor, M., Poloczanska, E., Mintenbeck, K., Nicolai, M., Okem, A., Petzold, J., Rama, B., Weyer, N. (Eds.), IPCC Special Report on the Ocean and Cryosphere in a Changing Climate.

Ishii, M., Shouji, A., Sugimoto, S., Matsumoto, T., 2005. Objective analyses of sea-surface temperature and marine meteorological variables for the 20th century using ICOADS and the Kobe Collection. Int. J. Climatol. 25, 865–879. https://doi.org/10.1002/joc.1169

Jiménez-Arias, J.L., Morris, E., Rubio-de-Inglés, M.J., Peralta, G., García-Robledo, E., Corzo, A., Papaspyrou, S., 2020. Tidal elevation is the key factor modulating burial rates and composition of organic matter in a coastal wetland with multiple habitats. Sci. Total Environ. 724. https://doi.org/10.1016/j.scitotenv.2020.138205

Jones, M.L.M., Sowerby, A., Williams, D.L., Jones, R.E., 2008. Factors controlling soil development in sand dunes: Evidence from a coastal dune soil chronosequence. Plant Soil 307, 219–234. https://doi.org/10.1007/s11104-008-9601-9

Kelleway, J.I., Saintilan, N., Macreadie, P.I., Baldock, J.A., Ralph, P.J., 2017. Sediment and carbon deposition vary among vegetation assemblages in a coastal salt marsh. Biogeosciences 14, 3763–3779. https://doi.org/10.5194/bg-14-3763-2017

Kemp, A.C., Vane, C.H., Horton, B.P., Culver, S.J., 2010. Stable carbon isotopes as potential sea-level indicators in salt marshes, North Carolina, USA. Holocene 20, 623–636. https://doi.org/10.1177/0959683609354302

Kemp, A.C., Vane, C.H., Horton, B.P., Engelhart, S.E., Nikitina, D., 2012. Application of stable carbon isotopes for reconstructing salt-marsh floral zones and relative sea level, New Jersey, USA. J. Quat. Sci. 27, 404–414. https://doi.org/10.1002/jqs.1561

Khan, N.S., Vane, C.H., Horton, B.P., 2015a. Stable carbon isotope and C/N geochemistry of coastal wetland sediments as a sea-level indicator. Handb. Sea-Level Res. 295–311. https://doi.org/10.1002/9781118452547.ch20

Khan, N.S., Vane, C.H., Horton, B.P., Hillier, C., Riding, J.B., Kendrick, C.P., 2015b. The application of δ13C, TOC and C/N geochemistry to reconstruct Holocene relative sea levels and paleoenvironments in the Thames Estuary, UK. J. Quat. Sci. 30, 417–433. https://doi.org/10.1002/jqs.2784

Kirwan, M.L., Megonigal, J.P., 2013. Tidal wetland stability in the face of human impacts and sea-level rise. Nature 504, 53–60. https://doi.org/10.1038/nature12856

Kirwan, M.L., Mudd, S.M., 2012. Response of salt-marsh carbon accumulation to climate change. Nature 488, 550–553. https://doi.org/10.1038/nature11440

Klap, V.A., Hemminga, M.A., Boon, J.J., 2000. Retention of lignin in seagrasses: Angiosperms that returned to the sea. Mar. Ecol. Prog. Ser. 194, 1–11. https://doi.org/10.3354/meps194001

Kuzyk, Z.Z.A., Goñi, M.A., Stern, G.A., Macdonald, R.W., 2008. Sources, pathways and sinks of particulate organic matter in Hudson Bay: Evidence from lignin distributions. Mar. Chem. 112, 215–229. https://doi.org/10.1016/j.marchem.2008.08.001

Lamb, A.L., Wilson, G.P., Leng, M.J., 2006. A review of coastal palaeoclimate and relative sea-level reconstructions using δ13C and C/N ratios in organic material. Earth-Science Rev. 75, 29–57. https://doi.org/10.1016/j.earscirev.2005.10.003

Legendre, P., Legendre, L., 2012. Numerical Ecology, 3rd editio. ed. Elsevier.

Li, Y., Von Storch, H., Wang, Q., Zhou, Q., Tang, S., 2019. Testing the validity of regional detail in global analyses of sea surface temperature - The case of Chinese coastal waters. Ocean Sci. 15, 1455–1467. https://doi.org/10.5194/os-15-1455-2019

Lueker, T.J., Dickson, A.G., Keeling, C.D., 2000. Ocean pCO2 calculated from dissolved inorganic carbon, alkalinity, and equations for K1 and K2: Validation based on laboratory measurements of CO2 in gas and seawater at equilibrium. Mar. Chem. 70, 105–119. https://doi.org/10.1016/S0304-4203(00)00022-0

Macreadie, K.R.P.I., Saintilan, J.J.K.N., 2019. Blue carbon in coastal landscapes : a spatial framework for assessment of stocks and additionality. Sustain. Sci. 14, 453–467. https://doi.org/10.1007/s11625-018-0575-0

Macreadie, P.I., Hughes, A.R., Kimbro, D.L., 2013. Loss of 'Blue Carbon' from Coastal Salt Marshes Following Habitat Disturbance. PLoS One 8, 1–8. https://doi.org/10.1371/journal.pone.0069244

Mariano, C., Marino, M., Pisacane, G., Sannino, G. , 2021. Sea Level Rise and Coastal Impacts: Innovation and Improvement of theLocal Urban Plan for a Climate-Proof Adaptation Strategy. Sustainability 13, 1565. https://doi.org/10.3390/su13031565
Mariotti, G., Carr, J., 2014. Dual role of salt marsh retreat: Long-term loss and short-term resilience. Water Resour. Res. 50, 50, 2963–2974. https://doi.org/10.1002/2013WR014676
Merloni, N., Piccoli, F., 1999. Carta della vegetazione - Parco regionale del Delta del Po - Stazione Pineta di San Vitale e Piallasse di Ravenna (Digitale) - Edizione 1999.
Meyers, P.A., 1994. Preservation of elemental and isotopic source identification of sedimentary organic matter. Chem. Geol. 114, 289–302. https://doi.org/10.1016/0009-2541(94)90059-0
Middelburg, J.J., Nieuwenhuize, J., Lubberts, R.K., Plassche, O. Van De, 1997. Organic Carbon Isotope Systematics of Coastal Marshes. Estuar. Coast. Shelf Sci. 45, 681–687.
Mollema, P., Antonellini, M., 2012. Climate and water budget change of a Mediterranean coastal. Env. Earth Sci 65, 257–276. https://doi.org/10.1007/s12665-011-1088-7
Mueller, P., Ladiges, N., Jack, A., Schmiedl, G., Kutzbach, L., Jensen, K., Nolte, S., 2019. Assessing the long-term carbon-sequestration potential of the semi-natural salt marshes in the European Wadden Sea. Ecosphere 10. https://doi.org/10.1002/ecs2.2556
Negandhi, K., Edwards, G., Kelleway, J.J., Howard, D., Safari, D., Saintilan, N., 2019. Blue carbon potential of coastal wetland restoration varies with inundation and rainfall. Sci. Rep. 1–9. https://doi.org/10.1038/s41598-019-40763-8
Oreska, M.P.J., Wilkinson, G.M., McGlathery, K.J., Bost, M., McKee, B.A., 2018. Non-seagrass carbon contributions to seagrass sediment blue carbon. Limnol. Oceanogr. 63, S3–S18. https://doi.org/10.1002/lno.10718
Ouyang, X., Lee, S.Y., 2014. Updated estimates of carbon accumulation rates in coastal marsh sediments. Biogeosciences 11, 5057–5071. https://doi.org/10.5194/bg-11-5057-2014
Palomo, L., Niell, F.X., 2009. Primary production and nutrient budgets of Sarcocornia perennis ssp. alpini (Lag.) Castroviejo in the salt marsh of the Palmones River estuary (Southern Spain). Aquat. Bot. 91, 130–136. https://doi.org/10.1016/j.aquabot.2009.04.002
Pendleton, L., Donato, D.C., Murray, B.C., Crooks, S., Jenkins, W.A., Megonigal, P., Pidgeon, E., Herr, D., Gordon, D., Baldera, A., 2012. Estimating Global ‘“ Blue Carbon ”’ Emissions from Conversion and Degradation of Vegetated Coastal Ecosystems. PLoS One 7, 1–7. https://doi.org/10.1371/journal.pone.0043542
Pisano, A., Buongiorno Nardelli, B., Tronconi, C., Santoleri, R., 2016. The new Mediterranean optimally interpolated pathfinder AVHRR SST Dataset (1982-2012). Remote Sens. Environ. 176, 107–116. https://doi.org/10.1016/j.rse.2016.01.019
Pisano, A., Marullo, S., Artale, V., Falcini, F., Yang, C., Leonelli, F.E., Santoleri, R., Nardelli, B.B., 2020. New evidence of Mediterranean climate change and variability from Sea Surface Temperature observations. Remote Sens. 12, 1–18. https://doi.org/10.3390/RS12010132
Ponti, M., Casselli, C., Abbiati, M., 2011. Anthropogenic disturbance and spatial heterogeneity of macrobenthic invertebrate assemblages in coastal lagoons: The study case of Pialassa Baiona (northern Adriatic Sea). Helgol. Mar. Res. 65, 25–42. https://doi.org/10.1007/s10152-010-0197-0
Preston, C.D., Pearman, A.D., Dines, D.T., 2002. New Atlas of the British and Irish Flora. Oxford University Press, Oxford.
Rayner, N.A., Parker, D.E., Horton, E.B., Folland, C.K., Alexander, L. V., Rowell, D.P., Kent, E.C., Kaplan, A., 2003. Global analyses of sea surface temperature, sea ice, and night marine air temperature since the late nineteenth century. J. Geophys. Res. D Atmos. 108, 1–22. https://doi.org/10.1029/2002jd002670
Rogers, K., Kelleway, J.J., Saintilan, N., Megonigal, J.P., Adams, J.B., Holmquist, J.R., Lu, M., Schile-beers, L., Zawadzki, A., Mazumder, D., Woodroffe, C.D., 2019. Wetland carbon storage controlled by millennialscale variation in relative sea-level rise. Nature 567, 91–96.
Roner, M., D’Alpaos, A., Ghinassi, M., Marani, M., Silvestri, S., Franceschinis, E., Realdon, N., 2016. Spatial variation of salt-marsh organic and inorganic deposition and organic carbon accumulation: Inferences from the Venice lagoon, Italy. Adv. Water Resour. 93, 276–287. https://doi.org/10.1016/j.advwatres.2015.11.011
Ruiz-fernández, A.C., Carnero-bravo, V., Sanchez-cabeza, J.A., Pérez-bernal, L.H., Amaya-monterrosa, O.A., 2018. Carbon burial and storage in tropical salt marshes under the in fl uence of sea level rise. Sci. Total Environ. 630, 1628–1640. https://doi.org/10.1016/j.scitotenv.2018.02.246
Saintilan, N., Rogers, K., Mazumder, D., Woodroffe, C., 2013. Allochthonous and autochthonous contributions to carbon accumulation and carbon store in southeastern Australian coastal wetlands. Estuar. Coast. Shelf Sci. 128, 84–92. https://doi.org/10.1016/j.ecss.2013.05.010
Sanchez-Cabeza, J.A., Ruiz-Fernandez, A.C., 2012. Pb sediment radiochronology : An integrated formulation and classification of dating models. Geochim. Cosmochim. Acta 82, 183–200.https://doi.org/10.1016/j.gca.2010.12.024
Simpson, L.T., Osborne, T.Z., Duckett, L.J., Feller, I.C., 2017. Carbon Storages along a Climate Induced Coastal Wetland Gradient. Wetlands 37, 1023–1035. https://doi.org/10.1007/s13157-017-0937-x
Sousa, A.I., Lillebø, A.I., Pardal, M.A., Caçador, I., 2010. The influence of Spartina maritima on carbon retention capacity in salt marshes from warm-temperate estuaries. Mar. Pollut. Bull. 61, 215–223. https://doi.org/10.1016/j.marpolbul.2010.02.018
Sousa, A.I., Santos, D.B., Silva, E.F. Da, Sousa, L.P., Cleary, D.F.R., Soares, A.M.V.M., Lillebø, A.I., 2017. ‘Blue Carbon’ and Nutrient Stocks of Salt Marshes at a Temperate Coastal Lagoon (Ria de Aveiro, Portugal). Sci. Rep. 7, 1–11. https://doi.org/10.1038/srep41225
Spivak, A.C., Sanderman, J., Bowen, J.L., Canuel, E.A., Hopkinson, C.S., 2019. Global-change controls on soil-carbon accumulation and loss in coastal vegetated ecosystems. Nat. Geosci. 12, 685–692. https://doi.org/10.1038/s41561-019-0435-2
Storto, A., Bonaduce, A., Feng, X., Yang, C., 2019. Steric Sea Level Changes from Ocean Reanalyses at Global and Regional Scales.

Water, 11(10), 1987. https://doi.org/10.3390/w11101987.
Tan, L., Ge, Z., Tang, J., Zhou, X., Li, S., Li, X., 2020. Conversion of coastal wetlands , riparian wetlands , and peatlands increases greenhouse gas emissions : A global 1638–1653. https://doi.org/10.1111/gcb.14933
Tanner, B.R., Uhle, M.E., Kelley, J.T., Mora, C.I., 2007. C3/C4 variations in salt-marsh sediments: An application of compound specific isotopic analysis of lipid biomarkers to late Holocene paleoenvironmental research. Org. Geochem. 38, 474–484. https://doi.org/10.1016/j.orggeochem.2006.06.009
Tanner, B.R., Uhle, M.E., Mora, C.I., Kelley, J.T., Schuneman, P.J., Lane, C.S., Allen, E.S., 2010. Comparison of bulk and compound-specific δ13C analyses and determination of carbon sources to salt marsh sediments using n-alkane distributions (Maine, USA). Estuar. Coast. Shelf Sci. 86, 283–291. https://doi.org/10.1016/j.ecss.2009.11.023
Tsimplis, M.N., Raicich, F., Fenoglio-marc, L., Shaw, A.G.P., Marcos, M., Somot, S., Bergamasco, A., 2012. Recent developments in understanding sea level rise at the Adriatic coasts. Phys. Chem. Earth 40–41, 59–71. https://doi.org/10.1016/j.pce.2009.11.007
USEPA, 2000. METHOD 6010C. INDUCTIVELY COUPLED PLASMA-ATOMIC EMISSION SPECTROMETRY. p. 30.
Van de Broek, M., Baert, L., Temmerman, S., Govers, G., 2019. Soil organic carbon stocks in a tidal marsh landscape are dominated by human marsh embankment and subsequent marsh progradation. Eur. J. Soil Sci. 70, 338–349. https://doi.org/10.1111/ejss.12739
Van De Broek, M., Temmerman, S., Merckx, R., Govers, G., 2016. Controls on soil organic carbon stocks in tidal marshes along an estuarine salinity gradient. Biogeosciences 13, 6611–6624. https://doi.org/10.5194/bg-13-6611-2016
Wakeham, S.G., Lee, C., Hedges, J.I., Hernes, P.J., Peterson, M.L., 1997. Molecular indicators of diagenetic status in marine organic matter. Geochim. Cosmochim. Acta 61, 5363–5369. https://doi.org/10.1016/S0016-7037(97)00312-8
Wang, F., Lu, X., Sanders, C.J., Tang, J., 2019. Tidal wetland resilience to sea level rise increases their carbon sequestration capacity in United States. Nat. Commun. 10, 1–11. https://doi.org/10.1038/s41467-019-13294-z
Ward, R.D., 2020. Carbon sequestration and storage in Norwegian Arctic coastal wetlands: Impacts of climate change. Sci. Total Environ. 748, 141343. https://doi.org/10.1016/j.scitotenv.2020.141343
Wilkinson, G.M., Besterman, A., Buelo, C., Gephart, J., Pace, M.L., 2018. A synthesis of modern organic carbon accumulation rates in coastal and aquatic inland ecosystems. Sci. Rep. 8, 1–9. https://doi.org/10.1038/s41598-018-34126-y
Wilson, G.P., 2017. On the application of contemporary bulk sediment organic carbon isotope and geochemical datasets for Holocene sea-level reconstruction in NW Europe. Geochim. Cosmochim. Acta 214, 191–208. https://doi.org/10.1016/j.gca.2017.07.038
Winogradow, A., Pempkowiak, J., 2014. Organic carbon burial rates in the Baltic Sea sediments. Estuar. , Coast. Shelf Sci. 138, 27–36.
World Bank, 2019. 'CO2 Emissions (Metric Tons Per Capita).' World Development Indicators.
Zerbini, S., Raicich, F., Maria, C., Bruni, S., Del, S., Errico, M., 2017. Earth-Science Reviews Sea-level change in the Northern Mediterranean Sea from long-period tide gauge time series 167, 72–87. https://doi.org/10.1016/j.earscirev.2017.02.009

933 Table 2. Carbon accummulation rates (g OC $m^{-2}$ $yr^{-1}$) in coastal wetlands in European Seas and worldwide averages.
934

| Area | type | time span | OC accumulation rate (g $m^{-2}$ $yr^{-1}$) | Dominant halophyte species/genera | Reference |
|---|---|---|---|---|---|
| Global (coastal and inland ecosystems) | sediment | <200 yr | 15.6 - 73.2 | *various* | (Wilkinson et al., 2018) |
| NW Atlantic | tidal wetlands soil | ca 100-150 yrs | 172.2±18.1 | *various* | (Ouyang and Lee, 2014) |
| US tidal wetlands | salt marsh sediments | nr[a] | 154.3±8 | *various* | (Wang et al., 2019) |
| ***NE Atlantic*** | | | | | |
| Norwegian Arctic coastal wetlands | low marsh | ca 100 yrs | 19-390 | *Juncus gerardii* | (Ward, 2020) |
| North Sea and Skagerrak Sea | continental shelf | ca 100 yrs | 0.02-66.18 | nr | (Diesing et al., 2021) |
| Baltic Sea | continental shelf, estuaries, fjords | nr | 13–54 | nr | (Winogradow and Pempkowiak, 2014) |
| Wadden Sea, Germany | semi-natural salt marsh | ca 50 yrs | 112-149 | *Spartina anglica, Salicornia europaea, Puccinellia maritima* | (Mueller et al., 2019) |
| Coastal margin habitats, UK | dry dune habitat | 140 yrs | 58±26 | *Carex arenaria, Hypochaeris radicata, Ammophila arenaria* | (Jones et al., 2008) |
| | wet dune habitat | 140 yrs | 73.0±22 | *Carex arenaria, Hypochaeris radicata, Ammophila arenaria* | (Jones et al., 2008) |
| | salt marsh | 60 yrs | 64-219 | nr | (Beaumont et al., 2014) |
| | machair | 60 yrs | 34.9±15.7 | nr | (Beaumont et al., 2014) |
| Blackwater Estuary, England | salt marsh | ca 10 yrs | 6.1-66 | *Salicornia* spp., *Spartina* spp., *Aster tripolium, Puccinellia maritima* | (Adams et al., 2012) |
| Scheldt estuary, Netherlands | salt marsh | <60 yrs | 88-151 | *E. athericus* | (Van De Broek et al., 2016) |

| | | | | | |
|---|---|---|---|---|---|
| | salt marsh | <60 yrs | 2177 ± 503 | *Spartina anglica* | (Van De Broek et al., 2016) |
| | salt marsh | <60 yrs | 22 ± 10 | *Mixed vegetation* | (Van De Broek et al., 2016) |
| | embanked salt marsh | <64 yr | 86.6± 7.5 | nr | (Van de Broek et al., 2019) |
| | embanked brackish marsh | ca 100 yrs | 111.3± 11.4 | nr | (Van De (Van de Broek et al., 2019) |
| Guadiana Estuary, Portugal | salt marsh | 13,000 - 6900 cal yrs BP | 164-314 | nr | (Boski et al., 2021) |
| Guadiana Estuary, Portugal | salt marsh | after 6900 cal yrs BP | 46-52 | nr | (Boski et al., 2021) |
| Mondego Estuary, Portugal | salt marsh | 2 yrs | <100 | *Scirpus maritimus* | (Couto et al., 2013) |
| | salt marsh | 2 yrs | 100-200 | *Spartina maritima* | (Couto et al., 2013) |
| | salt marsh | 2 yrs | 300-400 | *Zoostera nolti, Spartina maritima* | (Couto et al., 2013) |
| | salt marsh | 2 yrs | 213-218 | *Spartina maritima* | (Sousa et al., 2010) |
| Tagus Estuary, North East Atlantic | salt marsh | <100 yrs | 150-340 | *Spartina maritima, Halimione portulacoides* | (Caçador et al., 2004) |
| Ria de Aveiro, Portugal | low marsh | nr | 119.5 ± 5.3 | *Spartina maritima* | (Sousa et al., 2017) |
| Ria de Aveiro, Portugal | mid & high marsh | nr | 132.7 ± 5.8 | *Juncus maritimus* | (Sousa et al., 2017) |
| Ria de Aveiro, Portugal | mid & high marsh | nr | 157.3 | *Halimione portulacoides* | (Sousa et al., 2017) |
| Ria de Aveiro, Portugal | mid & high marsh | nr | 152 | *Sarcoconia perennis* | (Sousa et al., 2017) |

| | | | | | |
|---|---|---|---|---|---|
| Odiel marshes | salt marsh | 2-3 yrs | 104 | Spartina maritima | (Curado et al., 2013) |
| Bay of Cadiz, Spain | tidal coastal wetland | ca 100 yrs | 40-107 | *Spartina maritima, Zoostera nolstei* | (Jiménez-Arias et al., 2020) |
| Palomones Estuary | salt marsh | nr | 560 | *Sarcoconia perennis* | (Palomo and Niell, 2009) |
| ***Mediterranean Sea*** | | | | | |
| Venice lagoon, North Adriatic, Italy | salt marsh | nr | 132 | *Salicornia veneta, Spartina maritima, Limonium narbonense, Sarcocornia fruticosa, Juncus maritimus* | (Roner et al., 2016) |
| Rhone River Delta, France | riverine sites | 3 yrs | 357 | *Juncus maritimus, Phragmites australis, Scirpus lacustris, Scirpus litoralis* | (Hensel et al., 1999) |
| | marine sites | 3 yrs | 87.9 | *Arthrocnemum fruticosum, Halmione portulacoides, Suaeda fruticosa, Limonium vulgare* | (Hensel et al., 1999) |
| | impounded sites | 3 yrs | 72.1 | *Juncus maritimus, Arthrocnemum fruticosum* | (Hensel et al., 1999) |
| Ebro River Delta, Spain | tidal marsh | ca 3 yrs | 94-126 | *Pragmites australis, Tipha* spp. | (Calvo-Cubero et al., 2014) |
| | salt marsh | <100 yr | 39-293 | *Sarcoconia fruticosa* | (Fennessy et al., 2019) |
| | brackish mash | <100 yr | 32-495 | *Phragmites australis, Cladium mariscus, Juncus maritimus, Sarcocornia fructicosa, Scirpus maritimus, Spartina versicolor, Paspalum* spp. | (Fennessy et al., 2019) |

[a] nr: not reported